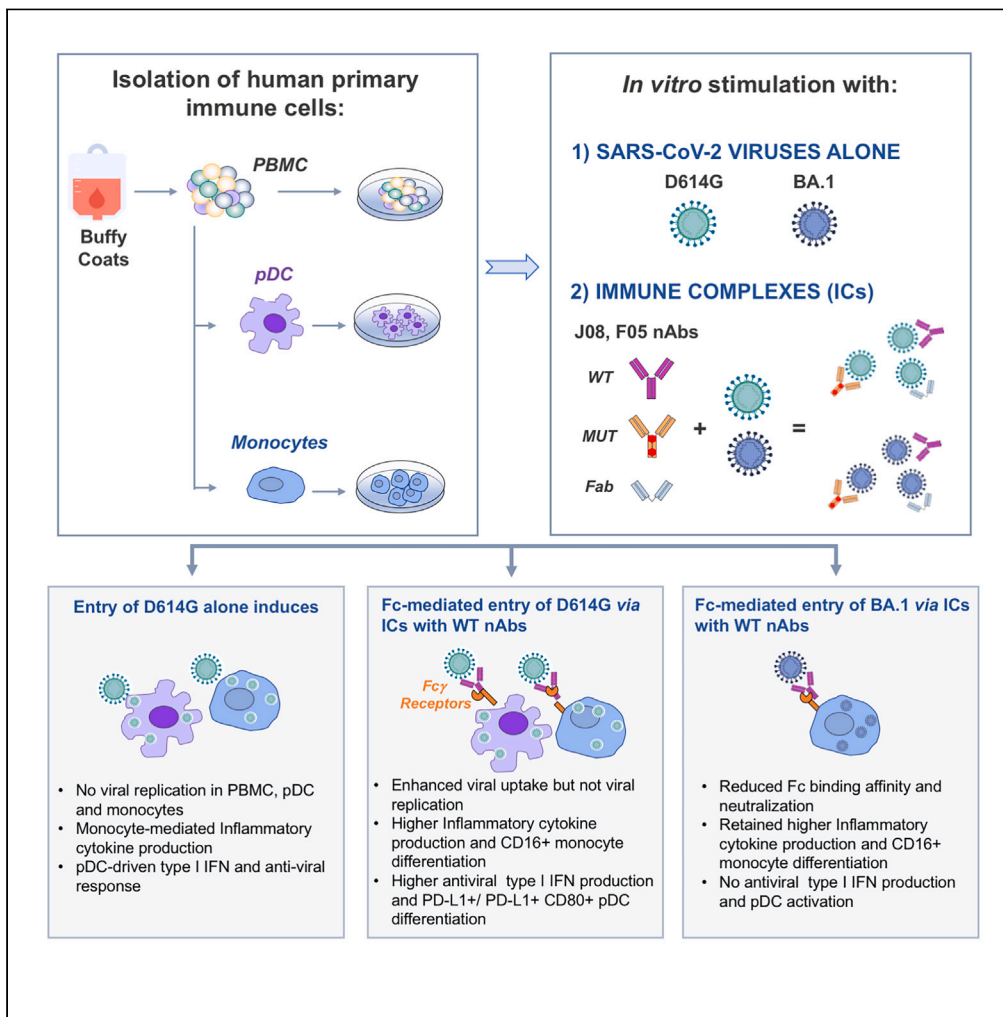


Article

Functional diversification of innate and inflammatory immune responses mediated by antibody fragment crystallizable activities against SARS-CoV-2



Martina Severa,
Marilena Paola
Etna, Emanuele
Andreano, ..., Rino
Rappuoli, Anna
Teresa Palamara,
Eliana Marina
Coccia

martina.severa@iss.it (M.S.)
eliana.coccia@iss.it (E.M.C.)

Highlights

Fc/FcR axis regulates inflammation and type I IFN in SARS-CoV-2-treated immune cells

Anti-Spike neutralizing Abs with WT Fc amplifies viral uptake, not replication

SARS-CoV-2+WT Ab immune complexes regulate monocyte and plasmacytoid DC phenotype

Omicron BA.1+WT Ab complexes promote IL6 release and CD16⁺ monocyte differentiation



Article

Functional diversification of innate and inflammatory immune responses mediated by antibody fragment crystallizable activities against SARS-CoV-2

Martina Severa,^{1,7,*} Marilena Paola Etna,^{1,7} Emanuele Andreano,² Daniela Ricci,^{1,3} Giada Cairo,¹ Stefano Fiore,¹ Andrea Canitano,⁴ Andrea Cara,⁴ Paola Stefanelli,¹ Rino Rappuoli,^{5,6} Anna Teresa Palamara,¹ and Eliana Marina Coccia^{1,8,*}

SUMMARY

Monoclonal antibodies (mAb) targeting the SARS-CoV-2 Spike (S) glycoprotein have been exploited for the treatment of severe COVID-19. In this study, we evaluated the immune-regulatory features of two neutralizing anti-S mAbs (nAbs), named J08 and F05, with wild-type (WT) conformation or silenced Fc functions.

In the presence of D614G SARS-CoV-2, WT nAbs enhance intracellular viral uptake in immune cells and amplify antiviral type I Interferon and inflammatory cytokine and chemokine production without viral replication, promoting the differentiation of CD16⁺ inflammatory monocytes and innate/adaptive PD-L1⁺ and PD-L1⁺CD80⁺ plasmacytoid Dendritic Cells. In spite of a reduced neutralizing property, WT J08 nAb still promotes the IL-6 production and differentiation of CD16⁺ monocytes once binding Omicron BA.1 variant.

Fc-mediated regulation of antiviral and inflammatory responses, in the absence of viral replication, highlighted in this study, might positively tune immune response during SARS-CoV-2 infection and be exploited also in mAb-based therapeutic and prophylactic strategies against viral infections.

INTRODUCTION

Moving from the success of monoclonal antibodies (mAbs) in the treatment of cancer, metabolic and autoimmune diseases,¹ mAb-based drugs and therapy have been deeply exploited during severe acute respiratory syndrome coronavirus 2 (SARS-CoV-2) pandemic, being deployed faster than antivirals and vaccines.² Targeting the Spike (S) protein of SARS-CoV-2, mAbs are used as a specific therapy in the outpatient setting for patients with mild-to-moderate disease precluding progression to a more severe course, especially for those categories of individuals that display multiple risk factors, including aged people or immunocompromised patients, such as those with cancer, transplant recipients or subjects taking immunosuppressant medications or with advanced cardiac, hepatic, or renal diseases.³ So far, a dozen of mAbs that target different epitopes and domains of the virus S protein have been approved for clinical use. Administered either individually, such as sotrovimab or bebtelovimab, or as combination therapy “cocktails,” such as Evusheld (cilgavimab + tixagevimab), mAbs have provided much-needed additional treatment options for the clinically vulnerable populations and for those who progress to severe disease.^{4,5} However, emerging SARS-CoV-2 variants have evaded most of mAbs approved for clinical application, and, having in mind the observation that SARS-CoV-2 variants resistant to mAb-based treatments can rapidly emerge in immunocompromised patients,⁶ the development of broadly applicable and potently variant-resistant neutralizing mAbs (nAbs) remains an unmet clinical need. Moreover, mAb-resistant variants could emerge and also manifest increased resistance to vaccine-induced immunity, thus representing a great challenge for the control of SARS-CoV-2 infection in the population.

Cellular entry of SARS-CoV-2 is mediated by the binding of the viral S protein to its cellular receptor, the angiotensin-converting enzyme 2 (ACE2), or to other host entry factors acting as co-receptors, including neuropilin-1 and TMPRSS2, involved in S protein maturation.^{7,8} Major goal of vaccine and therapeutic development is to generate nAbs that prevent SARS-CoV-2 entry into the cells by blocking either

¹Department of Infectious Diseases, Istituto Superiore di Sanità, 00161 Rome, Italy

²Monoclonal Antibody Discovery Lab, Fondazione Toscana Life Sciences, 53100 Siena, Italy

³Department of Sciences, Roma Tre University, 00154 Rome, Italy

⁴National Center for Global Health, Istituto Superiore di Sanità, 00161 Rome, Italy

⁵Department of Biotechnology, Chemistry and Pharmacy, University of Siena, 53100 Siena, Italy

⁶Fondazione Biocentro di Siena, 53100 Siena, Italy

⁷These authors contributed equally

⁸Lead contact

*Correspondence: martina.severa@iss.it (M.S.), eliana.coccia@iss.it (E.M.C.)

<https://doi.org/10.1016/j.isci.2024.109703>



ACE2-receptor binding domain (RBD) interactions or S-mediated membrane fusion, thus driving virus neutralization. Nonetheless, effector functions mediated by the constant Fragment crystallizable (Fc) portion of Abs, namely Ab-dependent cellular phagocytosis by monocytes (ADCP) and neutrophils (ADNP), Ab-dependent cell-mediated cytotoxicity (ADCC) or Ab-dependent complement deposition (ADCD), may represent a potential hurdle of mAb-based therapeutics. Although these innate immune functions are beneficial in the context of bacterial infection as they contribute to pathogen clearance, during infection with some classes of viruses these processes can exacerbate viral disease increasing infection rate and replication or induce inflammation and immunopathology by mediating immune complex (IC) formation. In particular, the risk of Ab-dependent enhancement (ADE) of diseases has been clearly demonstrated in the case of SARS-CoV, Respiratory Syncytial Virus and dengue viruses, and the theoretical risk has been raised, but then excluded, in the case of SARS-CoV-2.^{9–11} In respiratory infections, ADE belongs to the so-called enhanced respiratory disease (ERD), whose clinical manifestations are dependent to medical interventions (especially vaccines and mAb-based therapy). In addition to the mechanism involving Fc Receptor (FcR)-dependent activity and complement activation, ERD also includes manifestations such as cytokine cascades and local cell-mediated immunopathology leading to tissue cell death.⁹

The knowledge acquired in the last years on the immunological features of mAbs allowed to pinpoint novel engineering approaches to enhance the effector functions. In particular, in addition to modifications of the F(ab')₂ fragment (Fab) aimed at enhancing mAbs ability to bind their cognate antigen, Fc engineering was explored to improve mAb pharmacokinetics and effector functions, namely to tune/abrogate FcR binding and to extend the serum half-life, thus potentiating the therapeutic use of mAb also to face infectious diseases. In this context, it is peculiar to highlight that while mAbs against viral pathogens require the attenuation of Fc effector functions to limit possible ADE or ERD dysfunctions, Fc-mediated immune activities are indeed essential for phagocytosis, killing, and clearance of bacteria. Therefore, by introducing specific modification in the Fc region, mAbs can be tailored to stimulate the optimal immune response to microorganisms, thus representing a valid option for the treatment of different types of infectious diseases,¹² mainly induced by viral pathogens such as HIV, influenza, EBOLA, SARS and dengue viruses^{13–18} but also against multidrug-resistant bacteria infection.¹⁹

In the attempt to develop an experimental model to evaluate the immune-stimulatory features of mAbs and to study the Fc-mediated regulation of immunity in infection settings, here human peripheral blood mononuclear cells (PBMC) were employed to investigate the effects induced by IC formation between SARS-CoV-2 and highly potent anti-S nAbs, named J08 and F05.²⁰ We took advantage of the use of these nAbs that were expressed as full-length immunoglobulin G1 (IgG1) in their wild-type version (WT), engineered in their Fc region to abrogate FcγR binding (MUT version) or as Fab version, which was used as control.²¹

Our previous work reported that PBMC respond to SARS-CoV-2 stimulation by producing antiviral, pro-inflammatory cytokines and chemokines via Toll-like receptor (TLR) 7/8-dependent signaling.²² Here, we stimulated PBMC with SARS-CoV-2 in the presence of the WT versions of nAbs, retaining intact FcγR stimulatory capacity and able to amplify virus uptake into cells. SARS-CoV-2 immunocomplexed with WT nAbs drove higher levels of interferon- α (IFN- α), tumor necrosis factor- α (TNF- α), Interleukin-6 (IL-6), and IL-8 release, in the absence of viral replication, as compared to PBMC adsorbed with virus alone or with ICs formed with SARS-CoV-2 and both the MUT and Fab versions of nAbs.

To dissect the contribution of different immune cell populations concurring to Fc-mediated inflammatory response, we interrogated purified monocytes and plasmacytoid dendritic cells (pDC), being both sensitive to SARS-CoV-2 infection²² and expressing FcγRs.²³ Also in these contexts, an important impact of Fc modification on the nAbs' capacity to modulate both cytokine and chemokine production as well as activation and differentiation status of monocytes and pDC were observed.

SARS-CoV-2 variants, and in particular the Omicron lineage, evade infection- and vaccination-induced immunity and show resistance against the majority of developed mAb-based therapies.^{24,25} Nonetheless, despite reduced neutralization, Fc-dependent Ab effector functions are emerging as critical immune mechanisms to provide protection from variant infection and severe COVID-19 development.^{26,27}

Interestingly, Omicron BA.1 variant in the presence of the WT J08 nAb mediates Fc-dependent effector functions in monocytes leading to enhanced IL-6 production and increased differentiation of CD16⁺ expressing inflammatory subsets, despite the reduced neutralization capacity.

The findings of our study revealed the importance of Ab-mediated Fc effector functions and shed lights on the activation of innate/antiviral mechanisms, which are activated during SARS-CoV-2 infection, that could provide protection against variant infection and severe COVID-19.

RESULTS

Fragment crystallizable-fragment crystallizable receptor signal drives the amplification of the inflammatory response in human peripheral blood mononuclear cells stimulated with SARS-CoV-2 immunocomplexed with anti-S neutralizing monoclonal antibodies

In a previous work, we were able to isolate and characterize S protein-specific Abs from patients with SARS-CoV-2 convalescent with an extremely potent capacity to neutralize live virus during the first wave of virus epidemic in Italy in 2020.²¹ In this study, we applied an *in vitro* human PBMC-based experimental model to dissect the immune mechanisms mediated by two identified nAbs, named J08 and F05, in course of SARS-CoV-2 acute infection. J08 and F05 nAbs specifically bind the S1 RBD and show high neutralization potency against the original D614G SARS-CoV-2 virus.²¹ and then also against the emerged B.1.1.7 (Alpha), B.1.351 (Beta), P.1 (Gamma) and B.1.617.2 (Delta) variants.²⁸ These nAbs were expressed as full-length WT IgG1 and were then mutated in the Fc region to abrogate FcγR binding activity (MUT).²¹ A nAb version retaining the Fab fragment only was also tested as control (Fab). In particular, PBMC were adsorbed with D614G virus (at a multiplicity of infection, MOI, of 0.04) with or without incubation with three increasing doses of J08 and F05 nAbs in the WT, MUT, and Fab versions: one-tenth of the virus neutralizing dose assessed for both the nAbs with a 100% inhibitory concentration (IC₁₀₀) of 7.81 ng nAb/mL for

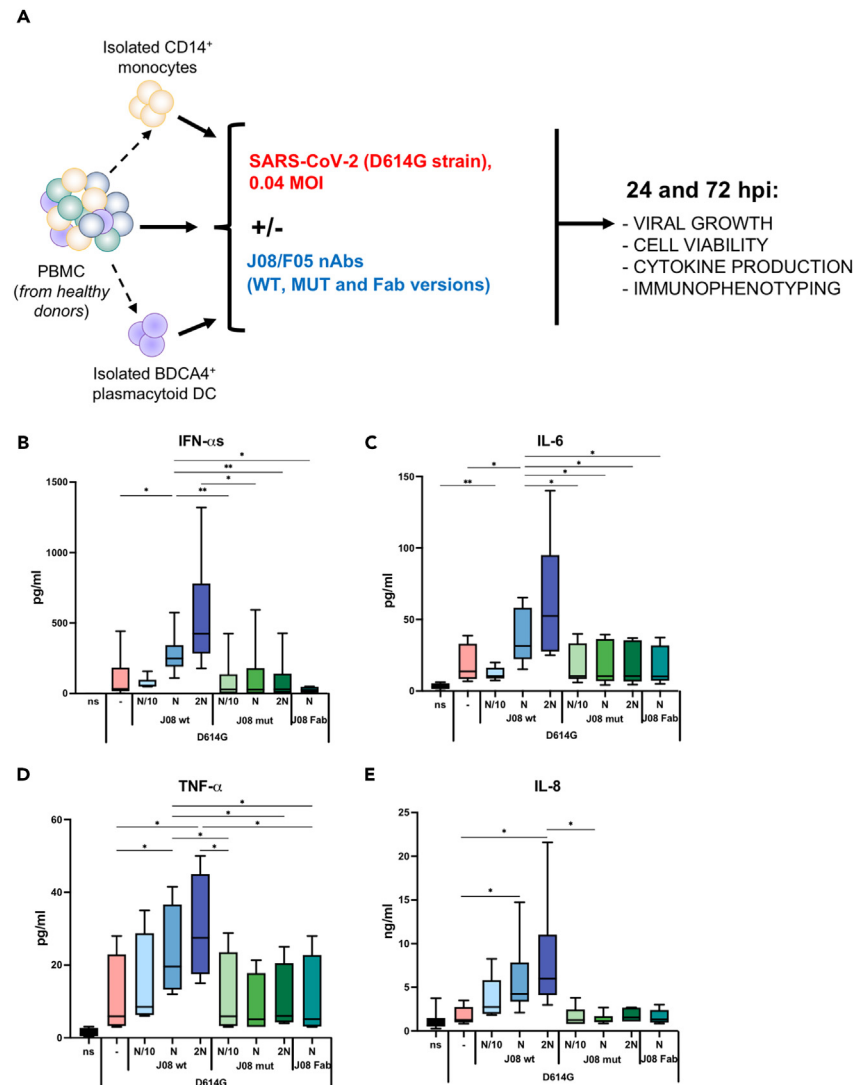


Figure 1. Inflammatory cytokine and chemokine production in PBMC treated with D614G virus in the presence of J08 nAbs

(A) Schematic representation of the *in vitro* experimental setting, culturing conditions and read-outs used in this study. Peripheral blood mononuclear cells (PBMC) and isolated CD14⁺ monocytes or BDCA4⁺ plasmacytoid dendritic cells (pDC) were collected from buffy coats of healthy volunteers. Cells were adsorbed for 1 hour (h) with D614G SARS-CoV-2 at 0.04 multiplicity of infection alone or after opsonization for 1 h with two classes of anti-SARS-CoV-2 Spike neutralizing IgG1 antibodies (nAbs) (i.e., J08 and F05), then cells were washed, and new complete medium added for cell culture. Cells were then analyzed at 24 or 72 h post-infection (hpi). J08 and F05 nAbs were used as wild-type version (WT), as a version engineered in the Fc receptor binding domain (MUT), as well as a version truncated in the complete constant Fc region (Fab). In particular, D614G SARS-CoV-2 was opsonized with three increasing doses of J08 and F05 nAbs in the WT, MUT, and Fab versions: one-tenth of the virus neutralizing dose assessed for both the nAbs at a concentration of 7.81 ng nAb/mL for 100 TCID₅₀ (Dose N/10), the neutralizing dose itself (Dose N) and twice the neutralizing dose (Dose 2N).

(B–E) PBMC isolated from healthy volunteers ($n = 8$) were left untreated (not stimulated, ns) or stimulated with D614G SARS-CoV-2 at a multiplicity of infection of 0.04 alone or in the presence of J08 nAbs in the WT, MUT, and Fab versions. Production of interferon (IFN)- α (B), as well as of the inflammatory cytokines interleukin (IL)-6 (C), tumor necrosis factor (TNF)- α (D) and the chemokine IL-8 (E) were measured in culture supernatants harvested at 24 (B) or 72 hpi (C–E). p -values were calculated by two-way ANOVA and assigned as follows: * ≤ 0.05 ; ** ≤ 0.01 .

100 TCID₅₀ of virus²⁰ (Dose N/10), the neutralizing dose itself (Dose N) and twice the neutralizing dose (Dose 2N) (Figure 1A). We have previously shown that human PBMC are not permissive to SARS-CoV-2 *in vitro* infection.²² Here, we firstly assess whether the complex of the D614G virus with WT, MUT, and Fab forms of J08 and F05 nAbs would impact viral replication in this experimental setting. Viral titration was performed at the inoculum check at time zero (T0), as well as at 24- and 72-h post-infection (hpi) (Figures S1A and S1B). Despite an unaltered cell viability in PBMC at the different experimental conditions in the presence of both J08 or F05 nAbs (Table 1), a sharp decrease was observed in viral titer measured in culture supernatants already at 24 hpi and that level was unchanged at 72 hpi, indicating no ongoing viral

Table 1. Rate of cell mortality in SARS-CoV-2-treated PBMC is not affected by adding of J08 and F05 nAbs

PBMC			
DEAD cells (% Fixable viability dye+ \pm SD)			
Cell culturing conditions	dose	24 hpi	72 hpi
ns		10.2 \pm 3	26.51 \pm 8
	J08 WT	N	11.2 \pm 4
	J08 MUT	N	9.6 \pm 1.8
	J08 Fab	N	9.5 \pm 0.2
	F05 WT	N	10.92 \pm 2
	F05 MUT	N	11.62 \pm 1
	F05 Fab	N	9.5 \pm 2
type C CpG	–	9.2 \pm 4	18.63 \pm 10
	J08 WT	N	8.6 \pm 0.8
	J08 MUT	N	8.5 \pm 1.2
R848	–	9.92 \pm 7	18.2 \pm 9
	J08 WT	N	7.79 \pm 2
	J08 MUT	N	8.58 \pm 2
D614G	–	8.31 \pm 10	18.3 \pm 9
	J08 WT	N/10	7.5 \pm 1
		N	8.8 \pm 8
		2N	9.4 \pm 0.3
	J08 MUT	N/10	8.49 \pm 0.1
		N	9.43 \pm 8.3
		2N	9.55 \pm 0.5
	J08 Fab	N	7.8 \pm 1
	F05 WT	N	7.9 \pm 7
	F05 MUT	N	10.4 \pm 0.5
	F05 Fab	N	9.5 \pm 0.2

Type C CpG: TLR-9 agonist (3 μ g/mL); R848: TLR-7/8 agonist (5 μ M); D614G SARS-CoV-2 strain (multiplicity of infection = 0.04).

J08/F05: anti-SARS-CoV-2 Spike neutralizing antibodies (nAb); WT: wild-type version of the nAb; MUT: Fc-mutated version of the nAb; Fab: Fab version of the nAb.

Hpi: hours post-infection.

N/10 = 1/10 neutralizing dose; N = neutralizing dose; 2N = twice the neutralizing dose.

replication (Figures S1A and S1B). These results further confirm that human PBMC are not permissive to SARS-CoV-2 infection and indicate that virus complexed with WT, MUT, and Fab versions of J08 or F05 nAbs does not induce *in vitro* viral replication.

Fc-FcR stimulation by Ab-virus ICs may amplify inflammation and cytokine production in Fc γ R-expressing immune cells. Thus, in culture supernatants of PBMC stimulated with SARS-CoV-2 alone or complexed with WT, MUT, and Fab J08 nAbs we evaluated the release of the antiviral IFN- α s, the inflammatory cytokines IL-6 and TNF- α , as well as the chemokine IL-8 (also named CXCL-8) (Figures 1B–1E). In the first set of experiments, we monitored these inflammatory mediators in kinetic at 24 and 72 hpi to assess the production peak *in vitro*. IFN- α s is rapidly released by stimulated PBMC and peaked at 24 hpi (Figure S2A), whereas IL-6, TNF- α and IL-8 showed their highest level at 72 hpi (Figures S2B–S2D), as also previously shown.²² So, these specific time points were used throughout the study to monitor the regulation of the different read-outs. When human PBMC were treated with D614G virus in the presence of WT J08 nAb, a dose-dependent dramatic increase in the release of all the analyzed soluble factors was observed as respect to what found in cultures treated with virus alone (Figures 1B–1E). The production levels remained, instead, unchanged when J08 MUT and Fab versions were used, indicating that Fc γ R-dependent mechanisms are needed to amplify SARS-CoV-2 mediated immune responses in immune cells (Figures 1B–1E). In line with these results, also in cultures stimulated with D614G in the presence of WT F05 an amplification of inflammation was found, while the presence of F05 MUT or Fab abolished the cytokine increment (Figures S3A–S3D). These findings were further corroborated by the fact that the adding of increasing concentration of WT, MUT, and Fab J08 or F05 nAbs to untreated PBMC cultures or in the presence of the TLR-9 ligand type C CpG oligodeoxynucleotides or the TLR7/8 ligand Resiquimod (R848) (Figures S4A–S4C or S4D–S4F, respectively) was not affecting cytokine

production, indicating that the increment in the inflammatory response observed in the presence of J08 or F05 WT nAbs occurs only upon their specific binding to SARS-CoV-2.

SARS-CoV-2 immunocomplexed with anti-S neutralizing monoclonal antibodies promotes Fc γ receptors crosslinking and Fc-mediated viral entry in peripheral blood mononuclear cells

To investigate the hypothesis that the crosslinking of FcR *per se* upon binding to ICs formed with SARS-CoV-2 and WT J08 nAb could drive antiviral/inflammatory cytokine response, we built up an *in vitro* experimental assay based on the stimulation of PBMC with streptavidin (SA)-labeled magnetic beads coated with biotinylated recombinant trimeric S protein then immunocomplexed with WT J08 nAb (Figure 2A). We found that, conversely to what was observed upon stimulation with WT J08 or S protein alone as well as WT J08 + S protein, the combination of WT J08 + S protein + beads, triggering FcR crosslinking, induces a strong production of the inflammatory mediators IL-6, TNF- α and IL-8 (Figures 2C–2E). Similar results were obtained when the crosslinking of all the Fc γ R expressed by immune cell subsets was obtained by stimulating as positive control PBMC with biotinylated goat anti-human CD16, CD32 and CD64 Abs coupled to SA-magnetic beads and then mixed together in equal quantity (Figures 2C–2E).

Nonetheless, no release of IFN- α s was detected upon FcR crosslinking *per se* (Figure 2B), differently to what was observed in PBMC stimulated with IC formed with WT J08 + live SARS-CoV-2 virus (see Figure 1B). Moreover, in the presence of IC with a live virus the stimulation of inflammatory cytokine production was much lower than that observed with the FcR crosslinking assay (compare Figures 1C–1E to 2C–2E), indicating that a modulation of cytokine production is occurring independently of FcR crosslinking.

Engagement of Fc-FcR mediated signals, indeed, may also enhance Ab-mediated virus uptake into Fc γ R-expressing immune cells amplifying innate response. To verify this hypothesis, we took advantage of virus-like particles (VLPs) containing green fluorescent protein (GFP) fused to Gag protein and pseudotyped with membrane-tethered D614G S protein alone or immunocomplexed with J08 nAbs in the WT or MUT versions (Figures 2F and 2G). Adsorption of PBMC with ICs formed with VLP-S and WT J08 doubled the percentage of GFP⁺ cells as compared to what was observed upon treatment with VLP-S only or ICs with VLP-S + MUT J08 (Figures 2F and 2G), demonstrating that WT J08 amplifies viral entry and uptake into Fc γ R-expressing cells.

Fragment crystallizable receptor signal drives the plasmacytoid dendritic cells diversification and amplification of type I interferon and inflammatory cytokine production in the presence of severe acute respiratory syndrome coronavirus 2 immunocomplexed with anti-S neutralizing monoclonal antibodies

Knowing that pDC are the main cell type producing type I IFN following viral infections and SARS-CoV-2 stimulation,²² we also studied their contribution to the immune response induced by SARS-CoV-2-containing ICs. Thus, pDC purified from PBMC of healthy volunteers were treated with D614G alone or in the presence of WT, MUT, and Fab J08 nAbs (Figure 3). We first assessed cell viability and viral replication in this pDC culture setting. No increment in cell mortality was found in the presence of nAbs (Table 2) and, in line with data obtained in PBMC, no increase in viral growth was observed at 24 hpi as compared to the inoculum check at time zero (T0) (Figure S1C). However, in D614G-stimulated pDC a strong production of IFN- α s, comparable to what found in PBMC, was detected, and the cytokine level was further increased in the presence of WT J08 only, corroborating the hypothesis that in this cell type a FcR-dependent amplification of viral entry is occurring potentiating cell stimulation (Figure 3A). In the same experimental conditions, an increment in the release of the inflammatory cytokine IL-6 (Figure 3B), TNF- α (Figure 3C), and the chemokine IL-8 (Figure 3D) was also observed.

pDC undergo phenotypical diversification in response to viral infections through environmental plasticity²⁹ and this was also observed upon SARS-CoV-2 stimulation.²² In particular, starting from PD-L1[−]CD80[−] resting P4-pDC they can diversify into three stable populations, namely PD-L1⁺CD80[−] innate P1-pDC specialized in type I IFN production, PD-L1⁺CD80⁺ P2-pDC displaying both innate and adaptive functions as well as specifically adaptive PD-L1[−]CD80⁺ P3-pDC (Figure S5A). By monitoring pDC immune phenotype in our experimental setting we found, as also previously reported,²² a clear-cut increase in the frequency of P1-pDC, in accordance with the detected high IFN- α release, upon D614G stimulation (Figures 3E and 3F). Nonetheless, the percentage of both P1 and P2 pDC subsets was importantly increased when cells were stimulated with virus in the presence of WT J08, but not with MUT or Fab nAbs (Figures 3E and 3F). In accordance with an induction of the adaptive functions of pDC along with the maturation process, the surface expression of the costimulatory marker CD86, normally used as indicator of an increased mature/activated status of cells, was strongly induced in the presence of D614G virus complexed with WT J08 as measured by MFI (Figures 3G and S5B). Furthermore, in these experimental conditions, we also assessed in pDC the surface level of the FcRs CD32 (or Fc γ RII) and CD64 (or Fc γ RI), whose expression is regulated in these cells in course of differentiation, and both resulted abundantly incremented (Figures 3G and S5C).

Fragment crystallizable receptor pathway amplifies the monocyte inflammatory response and differentiation in the presence of severe acute respiratory syndrome coronavirus 2 immunocomplexed with anti-S neutralizing monoclonal antibodies

To further dissect the different contributions of the main Fc γ R-expressing immune cell subsets to the anti-S nAb-regulated inflammatory response, we investigated the response of CD14⁺ monocytes purified from human PBMC. As seen, for whole PBMC and isolated pDC, the stimulation of monocytes with D614G virus alone or complexed with WT, MUT, and Fab J08 nAbs did not alter cell viability (Table 2) and did not induce viral replication (Figure S1D) either at 24 or at 72 hpi. The treatment of monocytes with D614G induces only a slight cytokine and chemokine production, while the stimulation with the virus opsonized with WT J08 nAb mediates an important increment in the

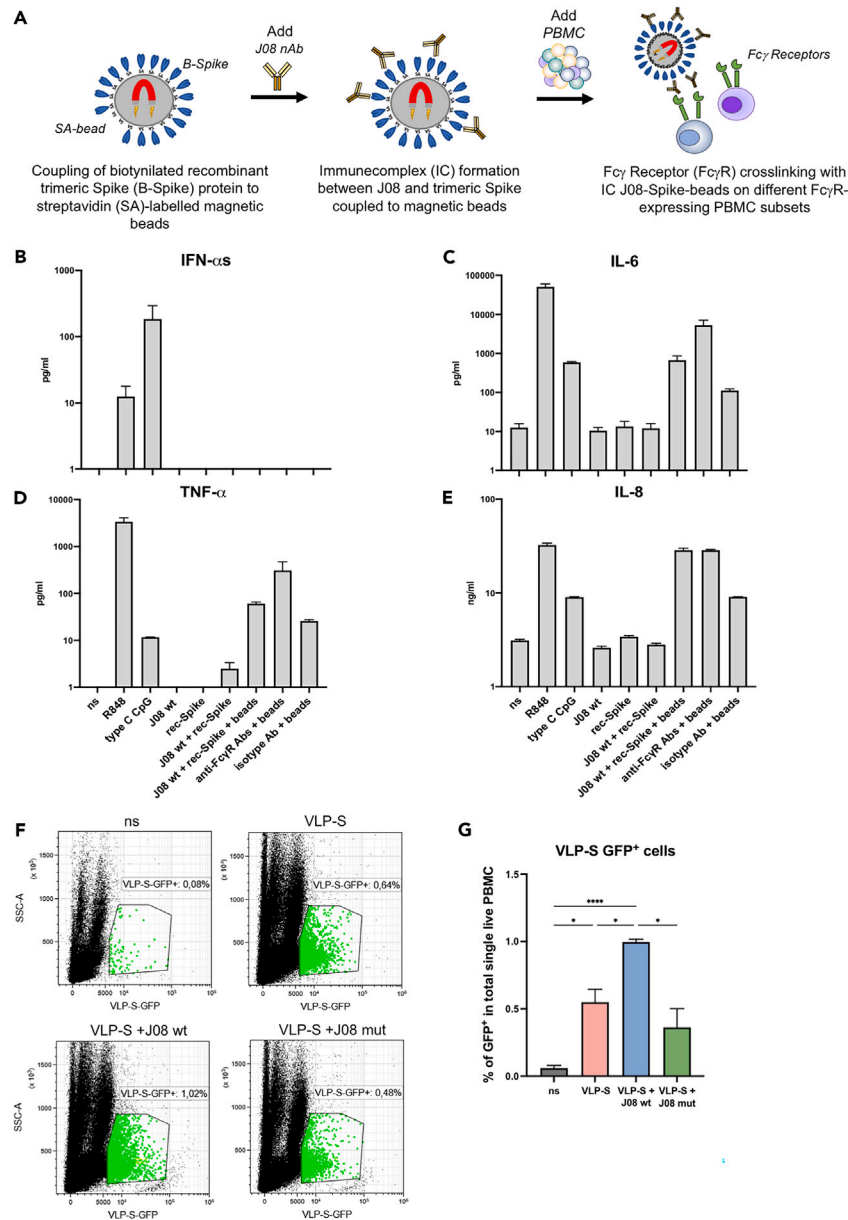


Figure 2. Fc γ R crosslinking with J08 nAb immune complexes and Fc-mediated viral entry in PBMC

(A) Schematic representation of the *in vitro* experimental setting used to mimic Fc γ R crosslinking. Biotinylated recombinant trimeric Spike (B-Spike) protein was coupled to streptavidin (SA)-labelled magnetic beads. Immune complexes (IC) were formed between anti-SARS-CoV-2 Spike neutralizing IgG1 antibody J08 in the wild-type (WT) version at the neutralizing dose and trimeric Spike coupled to SA-magnetic beads. IC were added to peripheral blood mononuclear cells (PBMC) to crosslink Fc γ Receptors (Fc γ R) on different Fc γ R-expressing PBMC subsets.

(B–E) PBMC isolated from healthy volunteers ($n = 3$) were left untreated (not stimulated, ns) or stimulated with J08 WT neutralizing antibody (nAb) and biotinylated recombinant (rec) trimeric Spike protein alone or coupled to SA-magnetic beads. As positive control biotinylated goat anti-human CD16, CD32 and CD64 antibodies (anti-Fc γ R Abs) were also coupled to SA-magnetic beads and then mixed together in equal quantity to crosslink all the Fc γ R expressed by PBMC subsets. Biotinylated goat anti-human immunoglobulin G (Isotype Ab) coupled to SA-magnetic beads was used as a negative control. Cells were also stimulated with the toll-like receptor (TLR)-7/8 agonist R848 and the TLR-9 agonist class C CpG. Production of interferon-alphas (IFN- α s) (B), interleukin (IL)-6 (C), tumor necrosis factor (TNF)- α (D) and IL-8 (E) was measured in culture supernatants.

(F and G) PBMC were adsorbed for 1 h with virus-like particles (VLP) expressing green-fluorescent protein (GFP) pseudotyped with membrane-tethered SARS-CoV-2 (D614G) Spike (S) protein alone or immunocomplexed with J08 nAbs in the WT or MUT versions. (F) Representative dot plots of the different experimental conditions derived from 1 experiment, out of 3 independently performed, are shown. (G) Results shown are the mean values of the percentage (%) of GFP $^+$ cells in total single live PBMC derived from the 3 experiments independently performed. *p*-values were calculated by two-way ANOVA and assigned as follows: * ≤ 0.05 ; **** ≤ 0.0001 .

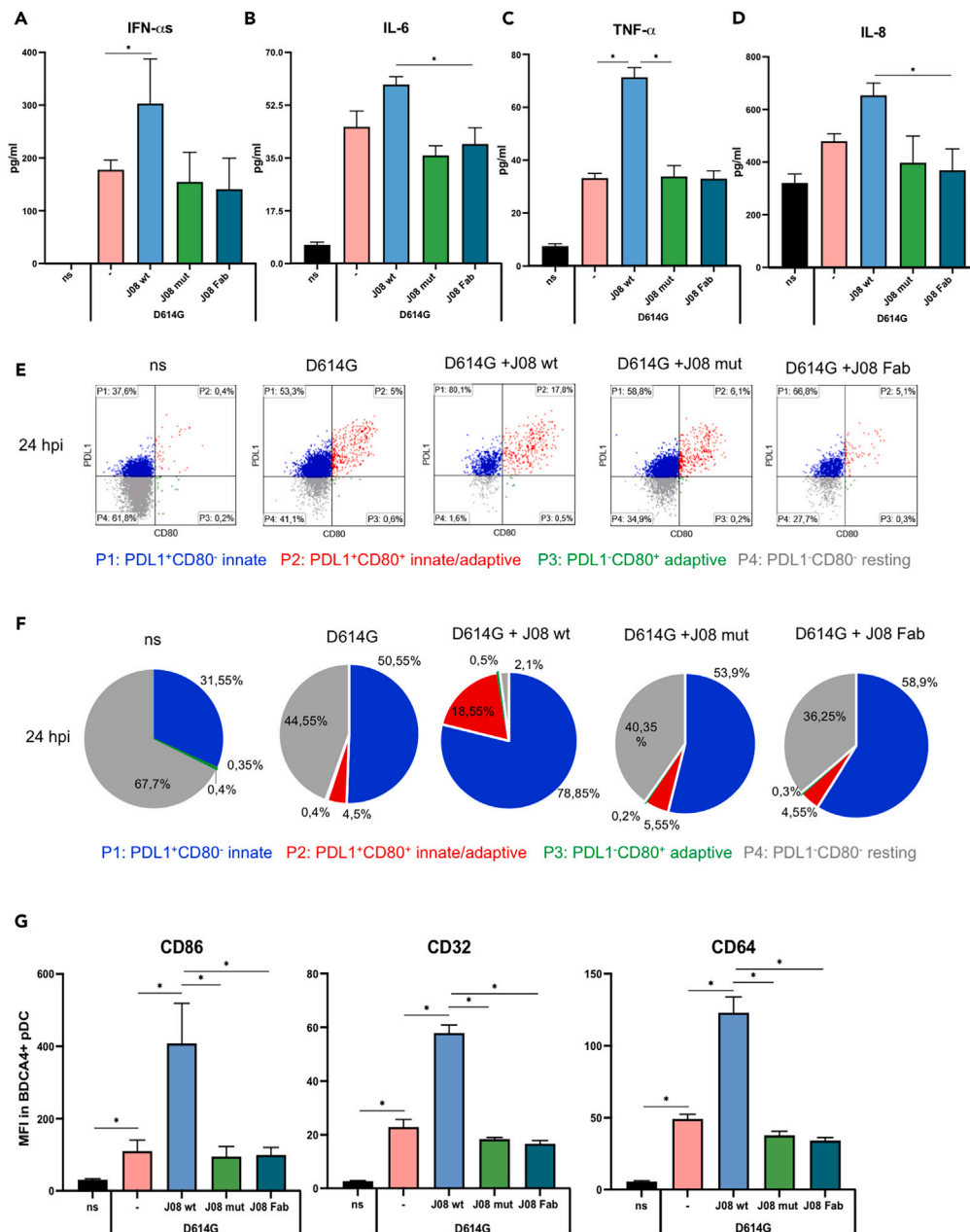


Figure 3. Regulation of cytokine release and immunophenotype in plasmacytoid dendritic cells treated with D614G in the presence of J08 nAbs

BDCA4⁺ plasmacytoid dendritic cells (pDC), purified from peripheral blood mononuclear cells (PBMC) of healthy volunteers ($n = 4$), were left untreated (not stimulated, ns) or stimulated with D614G virus at a multiplicity of infection of 0.04 alone or in the presence of the neutralizing dose of the anti-SARS-CoV-2 Spike neutralizing IgG1 antibody J08 in the wild-type (WT), Fc mutated (MUT) and Fc truncated (Fab) versions. Cells were harvested at 24 h post-infection (hpi). (A–D) Production of interferon-alphas (IFN- α s) (A) and the inflammatory cytokines interleukin (IL)-6 (B) and tumor necrosis factor (TNF)- α (C) as well as of the chemokine IL-8 (D) were measured in culture supernatants.

(E–G) pDC were studied by flow cytometry for cell subset differentiation. In particular, innate P1-pDC (PDL1⁺CD80⁻, in blue), innate/adaptive P2-pDC (PDL1⁺CD80⁺, in red), adaptive P3-pDC (PDL1⁻CD80⁺, in green) as well as resting P4-pDC (PDL1⁻CD80⁻, in gray) were analyzed. (E) Representative dot plots at the different experimental conditions displaying different pDC subsets derived from 1 experiment, out of 4 independently performed, are shown. (F) Results shown in the pie charts are mean values of the percentage (%) of the different pDC subsets analyzed in the parental single-live BDCA4⁺-gated cells in the 4 experiments independently performed. (G) Surface expression of the costimulatory marker CD86 as well as of the Fc receptors CD32 and CD64 was determined as mean fluorescence intensity (MFI) by cytofluorimetric analysis in single-live BDCA4⁺ pDC. Results were shown as median values \pm Interquartile range of 4 independent experiments. p -values were calculated by two-way ANOVA and assigned as follows: * ≤ 0.05 .

Table 2. Rate of cell mortality in SARS-CoV-2-treated isolated plasmacytoid dendritic cells and monocytes is not affected by adding of J08 nAb versions

Plasmacytoid Dendritic Cells (n = 4)

DEAD cells (% Mean Fixable viability dye+ ± SD)

Culturing conditions	dose	24hpi
ns		39.1 ± 5.80
Type C CpG	–	40.50 ± 12.02
D614G	–	40.70 ± 17.96
	J08 WT	N
	J08 MUT	N
	J08 Fab	N

Monocytes (n = 4)

DEAD cells (% Mean Fixable viability dye+ ± SD)

Culturing conditions	dose	24hpi	72hpi
ns		7.08 ± 3.43	22.40 ± 2.5
R848	–	8.38 ± 0.39	13.53 ± 5.8
D614G	–	6.45 ± 0.17	18.42 ± 14.7
	J08 WT	N	8.20 ± 1.79
	J08 MUT	N	8.10 ± 1.39
	J08 Fab	N	8.35 ± 3.45

Type C CpG: TLR-9 agonist (3 µg/mL); R848: TLR-7/8 agonist (µM); D614G SARS-CoV-2 strain (multiplicity of infection = 0.04).

Hpi: hours post-infection.

N = neutralizing dose.

J08: anti-SARS-CoV-2 Spike neutralizing antibody (nAb); wt: wild-type version of the nAb; MUT: Fc-mutated version of the nAb; Fab: Fab version of the nAb.

inflammatory response with a very robust release of IL-6, TNF- α , and IL-8 (Figures 4A–4C). This increment was abolished when viral stimulation was done in the presence of MUT or Fab versions of J08 resulting in a cytokine production that was similar to that observed in cultures untreated or treated with virus only. No release of IFN- α s was observed in any of the tested experimental conditions. Thus, we evaluated *in vitro* the immune phenotype of cultured monocytes upon exposure to D614G in the presence of WT, MUT or Fab J08 to define if the differentiation of inflammatory monocyte subsets would correlate with the observed hyper-inflammation, as previously shown *ex vivo* in different COVID-19 patient groups displaying diversified enrichment patterns of monocyte populations.^{30,31} The relative abundance of the different monocyte subpopulations carrying differential CD14 and CD16 expression levels was investigated (Figures 4D and 4E). In particular, we distinguished among three different subsets of circulating monocytes: namely the CD14^{hi}CD16^{neg} classical, the CD14⁺CD16^{int} intermediate/inflammatory, and the CD14^{low-neg}CD16^{hi} non-classical/atypical monocytes (Figure S6A). An important increase in the relative frequency of both CD14⁺CD16^{int} inflammatory and CD14^{low-neg}CD16^{hi} atypical subsets was found at 24 hpi when monocytes were exposed to D614G alone, as also previously reported by our group.³² Interestingly, the differentiation into inflammatory and atypical subpopulations was more pronounced when D614G complexed to WT J08 was added to cultures and this observation was even more sustained at 72 hpi (Figures 4D and 4E), coupling with the increase observed in the release of inflammatory mediators (see Figures 4A–4C). Conversely, when ICs were formed with virus and MUT or Fab J08 nAbs, results similar to that seen with virus alone were found (Figures 4D and 4E). Next, we also evaluated the activation status of monocytes by monitoring the expression of the costimulatory molecule CD86, as well as the surface levels of the different FcRs expressed by monocytes and regulated in course of differentiation, namely CD16 (or Fc γ RIII), CD32 (or Fc γ RII) and CD64 (or Fc γ RI). By comparing monocyte cultures at 24 and 72 hpi, we observed that the surface expression of CD86, as well as that of the studied FcRs, was strongly induced mainly at 72 hpi upon treatment with D614G alone (Figures 4F, S6B, and S6C). Nonetheless, at this time point levels of these markers were further amplified in the presence of WT J08nAb, while no effect was exerted by MUT and Fab J08 versions (Figures 4F, S6B, and S6C).

Overall, these data indicate that, when the D614G virus gets complexed with anti-S Abs, the FcR-dependent mechanism of viral entry can mediate and amplify the induction of inflammatory responses and immune diversification acting on specific immune cell subsets, such as monocytes and pDC.

Wild type J08 amplifies inflammatory cytokines and differentiation of the CD16⁺ monocyte also in the presence of omicron BA.1

Finally, we wanted to assess the capacity of J08 nAbs to mediate FcR-dependent immune responses also upon infection with Omicron BA.1 variant. Indeed, despite an important reduction in the IC₁₀₀ and IC₅₀, J08 nAb still retains some neutralization activity against this variant,

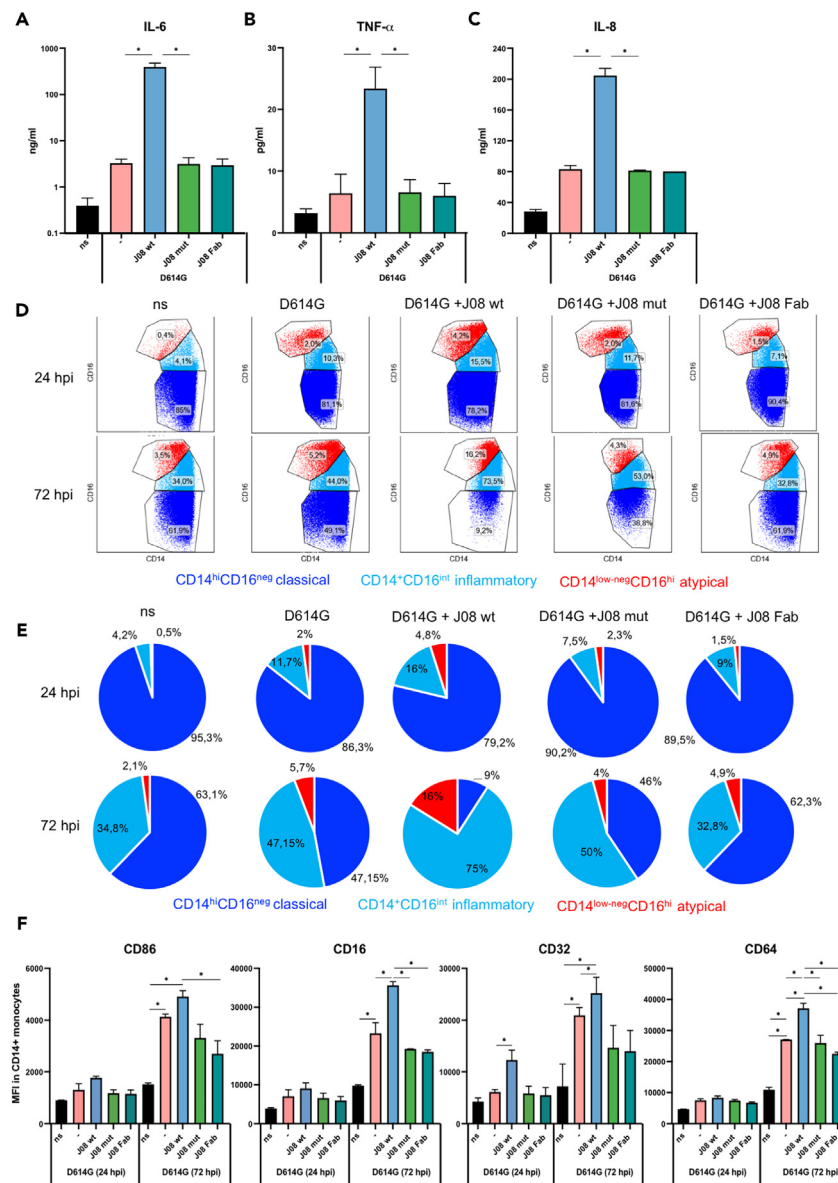


Figure 4. Regulation of cytokine release and immunophenotype in monocytes treated with D614G in the presence of J08 nAbs

CD14⁺ monocytes, purified from peripheral blood mononuclear cells (PBMC) of healthy volunteers ($n = 4$), were left untreated (not stimulated, ns) or stimulated with D614G virus at a multiplicity of infection of 0.04 alone or upon opsonization with the neutralizing dose of the anti-SARS-CoV-2 Spike neutralizing IgG1 antibody J08 in the wild-type (WT), Fc mutated (MUT) and Fc truncated (Fab) versions. Cells were harvested at 24 and 72 h post-infection (hpi).

(A–C) Production of the inflammatory cytokines interleukin (IL)-6 (A), tumor necrosis factor (TNF)- α (B) as well as of the chemokine IL-8 (C) were measured in culture supernatants.

(D–F) Monocytes were studied by flow cytometry for cell subset differentiation. In particular, classical [CD14^{hi}CD16^{neg}] monocytes are indicated in blue, inflammatory [CD14⁺CD16^{int}] monocytes in aqua blue, and atypical [CD14^{low-neg}CD16^{hi}] monocytes in red. (D) Representative dot plots at the different experimental conditions displaying different monocyte subsets derived from 1 experiment, out of 4 independently performed, are shown. (E) Results shown in the pie charts are mean values of the percentage (%) of the different monocyte subsets analyzed in the parental single-live CD14⁺-gated cells in the 4 experiments independently performed. (F) Surface expression of the costimulatory marker CD86 as well as of the Fc receptors CD16, CD32, and CD64 was determined as mean fluorescence intensity (MFI) by cytofluorimetric analysis in single-live CD14⁺ monocytes. Results were shown as median values \pm Interquartile range of 4 independent experiments. p -values were calculated by two-way ANOVA and assigned as follows: * ≤ 0.05 .

differently from other mAbs.²⁸ PBMC were adsorbed with Omicron BA.1 virus at a MOI of 0.04 in the presence or absence of J08 nAbs in the WT, MUT, and Fab forms (Figure 5A). Differently to what was observed with D614G, stimulation of PBMC with Omicron BA.1 complexed with WT J08 nAb impacts only on the release of IL-6 (Figure 5B), without influencing IFN- α s, TNF- α and IL-8 that remained unchanged as respect to what found either in the presence of MUT or Fab nAbs or in cultures stimulated with virus only (Figures S7A–S7C). Interestingly, in line with an

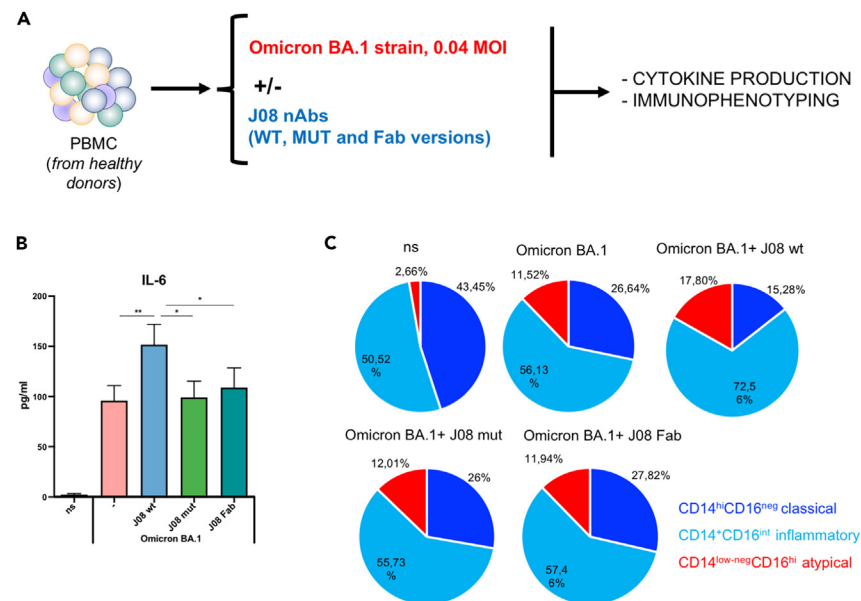


Figure 5. Impact of Omicron BA.1 infection on monocyte-driven inflammatory response in the presence of J08 nAbs

Peripheral blood mononuclear cells (PBMC) isolated from healthy volunteers ($n = 4$) were left untreated (not stimulated, ns) or stimulated for 24 or 72 h with Omicron BA.1 virus at a multiplicity of infection of 0.04 alone or upon opsonization with the neutralizing dose (N) of the anti-SARS-CoV-2 Spike neutralizing IgG1 antibody J08 (nAb) in the wild-type (WT), Fc mutated (MUT) and Fc truncated (Fab) versions.

(A) A schematic representation of experimental settings is depicted.

(B) Production of the inflammatory cytokine interleukin (IL)-6 was measured in culture supernatants harvested at 72 h post-infection. Results were shown as median values \pm Interquartile range of 4 independent experiments. p -values were calculated by two-way ANOVA and assigned as follows: * ≤ 0.05 ; ** ≤ 0.01 .

(C) Cells were harvested at 72 h post-infection and studied by flow cytometry for monocyte subset differentiation. In particular, classical [CD14^{hi}CD16^{neg}] monocytes are indicated in blue, inflammatory [CD14⁺CD16^{int}] monocytes in aqua blue, and atypical [CD14^{low-neg}CD16^{hi}] monocytes in red. Results shown in the pie charts are mean values of the percentage (%) of the different monocyte subsets analyzed in the parental single-live CD14⁺-gated cells in the 4 experiments independently performed.

increased IL-6 production, Omicron BA.1 in the presence of WT J08 also induced an enhanced differentiation of monocytes into inflammatory and atypical CD16-expressing subsets thus indicating the requirement of an intact FcR-dependent pathway to amplify monocyte responses in these conditions (Figure 5C).

DISCUSSION

Recent findings on COVID-19 and anti-SARS-CoV-2 mRNA-based vaccination, strongly support the vision that Fc-Fc γ R responses do not only mediate effector functions to control infection, but they also possess strong immune-regulatory features orchestrating cytokine production, regulating the response to mAb-based therapeutics and contributing to vaccine-induced Ab-mediated protection.

The therapeutic usage of anti-S glycoprotein mAbs in SARS-CoV-2 infection aims at preventing or reducing the risk of COVID-19 disease progression and occurrence of death, mainly in immunocompromised and fragile categories of patients, by blocking viral spread and infection. In a worldwide viral emergency crisis, such as that occurring during the COVID-19 pandemic, the possibility to complement immunization strategies with the passive administration of mAbs has been of key importance and it remains a useful tool in future emergency scenarios. Thus, understanding in depth the mechanisms behind the use of mAbs to exploit their application in either viral or bacterial infection and establishing new models to investigate these aspects in a pre-clinical setting are central to discriminate between positive therapeutic outcomes and potential hurdles.

To investigate the mechanisms behind the Fc effector functions to SARS-CoV-2 infection, we took advantage of two well-characterized anti-SARS-CoV-2 S glycoprotein nAbs named J08 and F05. Both nAbs were shown to bind the S RBD of SARS-CoV-2 and were engineered to abrogate the Fc binding to Fc γ Rs.^{21,24} Given its extreme neutralization potency and prophylactic and therapeutic activity *in vivo*, J08 was also developed and tested in phase I (EudraCT N.: 2020-005469-15 and [ClinicalTrials.gov](https://clinicaltrials.gov/ct2/show/study/NCT04932850) Identifier: NCT04932850) and phase II/III ([ClinicalTrials.gov](https://clinicaltrials.gov/ct2/show/study/NCT04952805) Identifier: NCT04952805) clinical trials, which were interrupted with the emergence of the first Omicron variant (BA.1).³³

In the PBMC-based *in vitro* model, we found that in the presence of D614G SARS-CoV-2, WT nAbs triggers Fc γ R crosslinking and enhances intracellular viral uptake in immune cells, without promoting viral replication. In these experimental conditions, the production of antiviral/inflammatory cytokines and chemokines was amplified in the presence of ICs with WT nAbs differently to what was observed in cultures stimulated with virus alone or with Fc-mutated and Fab versions of the nAbs, thus contributing to the establishment of a microenvironment

unfavorable to viral replication. Specifically, an enhanced release of the antiviral IFN- α , of the pro-inflammatory cytokines IL-6 and TNF- α and the neutrophil-chemoattractant molecule IL-8 was found.

Monocytes and pDC, two key cell types involved in antiviral and inflammatory responses employing the Fc-Fc γ R axis, released higher amounts of cytokines and chemokines and acquire a more activated phenotype only when exposed to D614G complexed with WT J08 nAb as respect to either the MUT or Fab J08 versions or the virus alone. In addition, an important increase in the relative frequency of both CD14⁺CD16^{int} inflammatory and CD14^{low-neg}CD16^{hi} atypical subsets was revealed when monocytes were exposed to SARS-CoV-2 alone, as also previously reported by our group in *in vitro* settings and in patients with COVID-19.³² Nonetheless, when in the presence of SARS-CoV-2 and WT J08, the differentiation into inflammatory and atypical subpopulations, producing the highest levels of inflammatory cytokines and chemokines, was even more pronounced. Similarly, pDC, that in response to viral stimulation undergo phenotypical diversification²⁹ as also seen upon SARS-CoV-2 exposure,²² displayed an increased frequency of the PD-L1⁺CD80⁻ innate P1 subset, specialized in type I IFN production, and PD-L1⁺CD80⁺ P2, with both innate and adaptive functions and able to produce high levels of IL-6 and TNF- α , in culture conditions containing the ICs with WT J08 as compared to the free virus or virus in complex with MUT or Fab nAbs. In monocytes and pDC cultures stimulated with D614G SARS-CoV-2 and the WT nAb, together with an increase in the activation and maturation status exemplified by the increased level of the costimulatory molecule CD86, also an enhanced surface expression of Fc γ RI (CD64) and Fc γ RII (CD32), as well as for monocytes also Fc γ RIII (CD16), was found, that can further amplify the Fc-Fc γ R mediated response upon stimulation with ICs formed with the WT nAbs.

The Fc γ R expression pattern is highly variable in different immune cell subsets in the resting state, as monocyte-derived DC express primarily Fc γ RIIa and Fc γ RIIb, macrophages and monocytes express multiple receptors (Fc γ RIa, Ila, I Ib, and IIIa), while pDC express Fc γ Rs only at very low levels.²³ Thus, it is likely that the FcR-mediated response observed in PBMC might represent the result of the cell type-specific composition in the Fc γ R repertoire since J08 and F05, being both IgG1, possesses the capacity to bind efficiently all Fc γ Rs.³⁴ Nevertheless, besides Fc γ Rs, other molecules expressed in myeloid cells can bind the Fc domain of Abs, such as the neonatal FcR (FcRn)³⁵ and Tripartite motif-containing protein 21 (TRIM21),³⁶ and they may partially contribute to the overall effects mediated by the binding of the ICs via the Fc portion. However, by comparing the effect induced by the J08 forms, which display different binding to FcRn, namely MUT J08 containing the two specific mutations abrogating Fc γ R binding and enhancing FcRn affinity²¹ and Fab J08 completely lacking the Fc portion, it is likely that in our setting the impact of FcRn is negligible.

All these data are suggestive of an important contribution of the Fc-Fc γ R axis, that in humans is crucial in controlling microbial infection,²³ in antiviral and inflammatory processes in the course of SARS-CoV-2 infection or vaccination. It has been already demonstrated that Fc γ R-mediated signals in human monocytes, macrophages, monocyte-derived DC, and pDC induces specific immune activation and specific cytokine and chemokine programs in different infection and autoimmunity settings. pDC were shown to exploit antigen uptake receptors such as Fc γ RIII (CD32) for the internalization of exogenous and opsonized antigens.³⁷ This mechanism, regulating the production of antiviral IFN- α and pro-inflammatory IL-6 and TNF- α as well as CD4⁺ and CD8⁺ T cell activation,^{38,39} was also taken into consideration for the generation of highly immune-stimulatory vaccines.⁴⁰ Also in monocytes, the recognition of opsonized microbes regulates cytokine production, besides mediating phagocytosis.^{23,41} In particular, in SARS-CoV-2 infection monocytes activate NLRP3 and AIM2 inflammasomes releasing inflammatory mediators upon uptake of Ab-opsonized virus by Fc γ Rs; this process induces pyroptotic cell death, thus, aborting the production of infectious virus but, in turn, causing systemic inflammation contributing to COVID-19 pathogenesis.⁴²

The emerging picture from these data indicates that human primary cells, such as PBMC, monocytes, and pDC, represent interesting settings to assess in *in vitro* pre-clinical studies the FcR-driven immune-stimulatory features mediated in the course of acute infections by IC formation between viruses and natural or vaccine-induced Abs or triggered by the administration of mAb-based therapeutics on the innate immune inflammatory response that needs to be evoked according to the target pathogen. In particular, if an induction of a pro-inflammatory response, against for instance antibiotic-resistant bacteria, is desired by exploiting the Fc-mediated effector functions of native mAbs, a dampened activation of FcR-expressing cells, such as monocytes or macrophages, is instead required to mitigate the risk of ADE by using mAbs engineered in the Fc γ R binding region. The scientific rationale to investigate innate immune cell response to mAbs relies on the crucial role that they exert in controlling *in vivo* the effects mediated by mAbs, such as the Fc-dependent effector functions including the release of cytokine and chemokines. The most common routes of mAb administration, namely intravenous or subcutaneous, deliver systemically mAbs via the blood vascular system or via the lymphatic system, respectively,⁴³ and, then, they can reach the infected tissues. In the inflamed tissues where immune cells are recruited to limit the infection, the formation of the IC between mAb and pathogen or pathogen-derived molecules triggers the Fc-mediated response against microorganisms. In this context, monocytes represent a key cell type involved in the control of natural infection in unvaccinated, vaccinated or mAb-treated subjects via the IC/FcR axis.^{30,42,44,45} Nevertheless, this implies the paradigm that opsonizing Abs contribute also to monocyte and macrophage infection and activation, thus sustaining an enhanced risk of ADE leading to deleterious immune reactions associated with severe disease.^{9,42} Indeed, in SARS-CoV-2 infection, it was shown that an increase in the formation of Fc γ RIII/CD16-reactive soluble ICs containing afucosylated, hyper-inflammatory IgG complexes might correlate with COVID-19 disease severity in predispose individuals.⁴⁶ These SARS-CoV-2-specific IgG with a pro-inflammatory phenotype together with abundant circulating ICs could greatly enhance, besides innate immune cells, also the high cytotoxic pathogenic potential of a particular subset of CD16⁺ expressing T cells found in acute and post-acute COVID-19 shown to be strongly activated by complement deposition and to drive lung microvascular endothelial cell activation.⁴⁷

Nonetheless, although the risk of ADE has been actively investigated in COVID-19 immunopathology, its occurrence in human SARS-CoV-2 diseases has been excluded or only partially hypothesized so far.^{9,48} Neither ADE of infection nor the enhancement of innate immune response was observed in monocyte-derived macrophages infected with SARS-CoV-2 opsonized by serum from patients with convalescent

COVID-19.⁴⁸ In line with these data, Junqueira and collaborators demonstrated that vaccine recipient plasma did not enhance Ab-dependent monocyte infection, indicating that ADE does not represent a risk also respect to vaccination.⁴² Occurrence of ADE was also investigated in people treated with approved therapeutic Ab drugs retaining an intact Fc portion and no increase but rather a decrease in SARS-CoV-2 viral load was reported.^{49–52}

Our results showed an amplified viral uptake in immune cells upon stimulation with ICs composed of WT nAbs and virus in the presence of an intact FcγR signal; however, no increase in viral replication was reported.

Moreover, during viral infections, such as dengue virus, MERS, and SARS-CoV, inducing intrinsic ADE, the antiviral response gets disabled by FcγR interaction with the IC activating an immune suppressive response by expressing IL-6, TNF-α, and IL-10 and by downregulating the expression of type I IFNs, resulting in increased virion production in the infected cells.^{53,54} Conversely, in our study we highlighted a Fc-mediated enhanced IFN-αs production mediated by pDC activation that might be able to tune antiviral responses and amplify viral clearance at the site of infection where immune cells expressing FcR are recruited.

Nevertheless, the development of Ab-based vaccines and therapeutics was influenced by the initial ADE concern and most of the neutralizing mAbs, that have been developed for the use in COVID-19 therapy, have been engineered to alter the binding capacity to FcγRs. This vision is, however, likely going to change in light also of work by Mackin and colleagues showing that serum Abs elicited by vaccines against the ancestral Wuhan-1 virus may still confer protection against infection by antigenically shifted SARS-CoV-2 variants, including Omicron strains.²⁶ These mechanisms involving the Fc-FcγR engagement mediate antiviral activity and enhanced effector functions in alveolar macrophages, thus improving clinical COVID-19 outcome, in the absence of ADE.²⁶ Interestingly, in line with this evidence, we proved that Omicron BA.1 strain complexed with WT J08 nAb still mediates an enhanced release of the inflammatory cytokine IL-6 impacting also on the differentiation of both CD14⁺CD16^{int} inflammatory and CD14^{low-neg}CD16^{hi} atypical monocyte subsets. Even in the presence of a reduced neutralization capacity against Omicron BA.1 of J08 nAbs and of a more rapid dissociation of the virus-mAb complex,²⁸ collectively these results suggest the requirement for Fc-mediated effector activities to protect vaccine recipients against severe COVID-19 induced by Omicron viruses in the setting of waning serum Ab neutralization.²⁶ Growing evidence, indeed, indicate that Fc-mediated Ab effector functions are crucial for protection against severe SARS-CoV-2 infection. Recently, we showed that mAbs with reduced neutralization capacity are able to induce strong and variant-resistant Fc-dependent functional responses, including complement deposition and phagocytosis.⁵⁵ From this perspective and based on our data showing a strong activation via Fc-FcγR axis of two crucial players of innate immunity against viruses, namely monocytes and pDC, a more broadly protective immune response could be achieved by the WT J08 nAb, that, even if only partially neutralizing the emerging variant,²⁸ could still elicit Fc effector functions thus opening new options and avenues for Ab-based therapeutics against SARS-CoV-2 emerging variants. Nonetheless, in this study we did not take into consideration the most recently circulating variants; however, recent evidences demonstrate that the binding of the anti-S mAb full-length IgG sotrovimab, which binds to all Omicron variants with different efficiency, confer protection against the BQ1.1 and XBB.1 variants promoting Fc-dependent effector functions.⁴⁵

Interestingly, our study also shows that FcR crosslinking induced by the stimulation of PBMC with ICs formed by the combination of WT J08 and S protein and SA-beads induces a strong production of the inflammatory mediators IL-6, TNF-α and IL-8. These results are in line with recent literature reporting a role for the SARS-CoV-2 S protein *per se*, independently of viral entry into cells, in the induction of inflammation leading to the disruption of vascular endothelial barrier and endotheliitis in severe COVID-19 via ACE-2 recognition and Integrin α5β1 signaling.^{56,57}

These mechanisms could also be linked to the so-called “Spike-hypothesis” during mRNA vaccination, that supposes a role for the tissue deposition or the systemic availability of encoded S protein in the induction of pro-inflammatory responses leading to vaccine adverse events.^{58,59} Based on our data, S-induced inflammation could also be triggered by IC formation between produced vaccine-specific Abs and vaccine-encoded S protein in an ACE-2-independent Fc-FcR-dependent mechanism.

More generally, findings from this study demonstrate the central importance of the Fc-FcγR axis that may regulate and potentiate antiviral and inflammatory responses in the course of SARS-CoV-2 infection and also suggest that this signal could be exploited and give indications for modeling in different infection settings or for studying protective responses induced by Ab-based therapeutic and prophylactic strategies against viral infections.

Limitations of the study

While in this study we described the Fc-mediated regulation of antiviral and inflammatory responses of two well-characterized and extremely potent anti-SARS-CoV-2 S nAbs, we did not compare it, with other commercially available mAbs. Nonetheless, since the number of approved therapeutic mAbs continuously evolves, it would be unfeasible to include all of them in our study.

Another limitation of our research is that we conducted only the *in vitro* characterization of Fc-mediated response in PBMC cultures and did not investigate *in vivo* in animal models the impact of the IC-mediated amplified antiviral response on viral clearance and protection. However, also the use of animal models can never fully predict efficacy or reproducibility in humans. Moreover, we do not know whether this phenomenon can be also driven by ICs formed in other viral infection settings or if this is a SARS-CoV-2-specific feature.

STAR★METHODS

Detailed methods are provided in the online version of this paper and include the following:

- [KEY RESOURCES TABLE](#)

- **RESOURCES AVAILABILITY**
 - Lead contact
 - Materials availability
 - Data and code availability
- **EXPERIMENTAL MODEL AND STUDY PARTICIPANT DETAILS**
 - Primary cultures of human origin
 - Vero E6 cells
 - 293T Lenti-X cells
 - Viral strains
- **METHOD DETAILS**
 - Isolation of PBMC, pDC and monocytes
 - Virus production and titration
 - Production and titration of VLPs
 - Cell stimulation
 - Viral uptake
 - FcR crosslinking assay
 - Detection of cytokines and chemokines in culture supernatants
 - Flow cytometric analysis
- **QUANTIFICATION AND STATISTICAL ANALYSIS**

SUPPLEMENTAL INFORMATION

Supplemental information can be found online at <https://doi.org/10.1016/j.isci.2024.109703>.

ACKNOWLEDGMENTS

The authors acknowledge Valentina Tirelli and the Flow Cytometry Facility (FAST) of Istituto Superiore di Sanità (Rome, Italy) for technical support.

This research was supported by EU funding within the MUR PNRR Extended Partnership initiative on Emerging Infectious Diseases (Project no. PE00000007, INF-ACT to CEM, EMP, SP, PAT) and by the Italian Ministry of Health (RIPrEl project, L106/2021).

AUTHOR CONTRIBUTIONS

SM: Conceptualization; data curation; investigation; methodology; project administration; visualization; writing – original draft; writing – review and editing. EMP: Data curation; investigation; methodology. AE: Conceptualization; data curation; methodology; writing – review and editing. RD, CG, Canitano A: Data curation; formal analysis; visualization; investigation. FS: investigation; methodology. Cara A, SP: methodology, writing – review and editing. RR: Conceptualization; methodology, writing – review and editing. PAT: Conceptualization; funding acquisition; writing – review and editing. CEM: Conceptualization; funding acquisition; project administration; supervision; validation; writing – review and editing.

DECLARATION OF INTERESTS

SM, EMP, RD, CG, Canitano A, Cara A, FS, SP, PAT, and CEM declare no conflict of interest.

AE and RR are listed as inventors of full-length human monoclonal antibodies described in Italian patent applications n. 102020000015754 filed on June 30th 2020, 102020000018955 filed on August 3rd 2020 and 102020000029969 filed on 4th of December 2020, and the international patent system number PCT/IB2021/055755 filed on the 28th of June 2021. All patents were submitted by Fondazione Toscana Life Sciences, Siena, Italy.

Received: August 8, 2023

Revised: January 25, 2024

Accepted: April 6, 2024

Published: April 11, 2024

REFERENCES

1. Berger, M., Shankar, V., and Vafai, A. (2002). Therapeutic applications of monoclonal antibodies. *Am. J. Med. Sci.* 324, 14–30. <https://doi.org/10.1097/00000441-200207000-00004>.
2. Kelley, B., De Moor, P., Douglas, K., Renshaw, T., and Traviglia, S. (2022). Monoclonal antibody therapies for COVID-19: lessons learned and implications for the development of future products. *Curr. Opin. Biotechnol.* 78, 102798. <https://doi.org/10.1016/j.copbio.2022.102798>.
3. Hirsch, C., Park, Y.S., Piechotta, V., Chai, K.L., Estcourt, L.J., Monsef, I., Salomon, S., Wood, E.M., So-Osman, C., McQuilten, Z., et al. (2022). SARS-CoV-2-neutralising monoclonal antibodies to prevent COVID-19. *Cochrane Database Syst. Rev.* 6, CD014945. <https://doi.org/10.1002/14651858.CD014945.pub2>.
4. Savoldi, A., Morra, M., De Nardo, P., Cattelan, A.M., Mirandola, M., Manfrin, V., Scotton, P.,

- Giordani, M.T., Brollo, L., Panese, S., et al. (2022). Clinical efficacy of different monoclonal antibody regimens among non-hospitalised patients with mild to moderate COVID-19 at high risk for disease progression: a prospective cohort study. *Eur. J. Clin. Microbiol. Infect. Dis.* 41, 1065–1076. <https://doi.org/10.1007/s10096-022-04464-x>.
5. Savoldi, A., Morra, M., Castelli, A., Mirandola, M., Berkell, M., Smet, M., Konnova, A., Rossi, E., Cataudella, S., De Nardo, P., et al. (2022). Clinical Impact of Monoclonal Antibodies in the Treatment of High-Risk Patients with SARS-CoV-2 Breakthrough Infections: The ORCHESTRA Prospective Cohort Study. *Biomedicines* 10, 2063. <https://doi.org/10.3390/biomedicines10092063>.
 6. Casadevall, A., and Focosi, D. (2023). SARS-CoV-2 variants resistant to monoclonal antibodies in immunocompromised patients constitute a public health concern. *J. Clin. Invest.* 133, e168603. <https://doi.org/10.1172/JCI168603>.
 7. Hoffmann, M., Kleine-Weber, H., Schroeder, S., Krüger, N., Herrler, T., Erichsen, S., Schiergens, T.S., Herrler, G., Wu, N.H., Nitsche, A., et al. (2020). SARS-CoV-2 Cell Entry Depends on ACE2 and TMPRSS2 and Is Blocked by a Clinically Proven Protease Inhibitor. *Cell* 181, 271–280.e8. <https://doi.org/10.1016/j.cell.2020.02.052>.
 8. Cantuti-Castelvetri, L., Ojha, R., Pedro, L.D., Djannatian, M., Franz, J., Kuivaneen, S., van der Meer, F., Kallio, K., Kaya, T., Anastasina, M., et al. (2020). Neuropilin-1 facilitates SARS-CoV-2 cell entry and infectivity. *Science* 370, 856–860. <https://doi.org/10.1126/science.abd2985>.
 9. Lee, W.S., Wheatley, A.K., Kent, S.J., and DeKosky, B.J. (2020). Antibody-dependent enhancement and SARS-CoV-2 vaccines and therapies. *Nat. Microbiol.* 5, 1185–1191. <https://doi.org/10.1038/s41564-020-00789-5>.
 10. Katzelnick, L.C., Gresh, L., Halloran, M.E., Mercado, J.C., Kuan, G., Gordon, A., Balmaseda, A., and Harris, E. (2017). Antibody-dependent enhancement of severe dengue disease in humans. *Science* 358, 929–932. <https://doi.org/10.1126/science.aan6836>.
 11. Arvin, A.M., Fink, K., Schmid, M.A., Cathcart, A., Spreafico, R., Havenar-Daughton, C., Lanzavecchia, A., Corti, D., and Virgin, H.W. (2020). A perspective on potential antibody-dependent enhancement of SARS-CoV-2. *Nature* 584, 353–363. <https://doi.org/10.1038/s41586-020-2538-8>.
 12. Grace, P.S., Gunn, B.M., and Lu, L.L. (2022). Engineering the supernatural: monoclonal antibodies for challenging infectious diseases. *Curr. Opin. Biotechnol.* 78, 102818. <https://doi.org/10.1016/j.copbio.2022.102818>.
 13. Zhou, T., Georgiev, I., Wu, X., Yang, Z.Y., Dai, K., Finzi, A., Kwon, Y.D., Scheid, J.F., Shi, W., Xu, L., et al. (2010). Structural basis for broad and potent neutralization of HIV-1 by antibody VRC01. *Science* 329, 811–817. <https://doi.org/10.1126/science.1192819>.
 14. Lingwood, D., McTamney, P.M., Yassine, H.M., Whittle, J.R.R., Guo, X., Boyington, J.C., Wei, C.J., and Nabel, G.J. (2012). Structural and genetic basis for development of broadly neutralizing influenza antibodies. *Nature* 489, 566–570. <https://doi.org/10.1038/nature11371>.
 15. Robinson, L.N., Tharakaraman, K., Rowley, K.J., Costa, V.V., Chan, K.R., Wong, Y.H., Ong, L.C., Tan, H.C., Koch, T., Cain, D., et al. (2015). Structure-Guided Design of an Anti-dengue Antibody Directed to a Non-immunodominant Epitope. *Cell* 162, 493–504. <https://doi.org/10.1016/j.cell.2015.06.057>.
 16. Sarker, A., Rathore, A.S., Khalid, M.F., and Gupta, R.D. (2022). Structure-guided affinity maturation of a single-chain variable fragment antibody against the Fu-bc epitope of the dengue virus envelope protein. *J. Biol. Chem.* 298, 101772. <https://doi.org/10.1016/j.jbc.2022.101772>.
 17. Wrotniak, B.H., Garrett, M., Baron, S., Sojar, H., Shon, A., Asiago-Reddy, E., Yager, J., Kalams, S., Croix, M., and Hicar, M.D. (2022). Antibody dependent cell cytotoxicity is maintained by the unmutated common ancestor of 6F5, a Gp41 conformational epitope targeting antibody that utilizes heavy chain VH1-2. *Vaccine* 40, 4174–4181. <https://doi.org/10.1016/j.vaccine.2022.05.083>.
 18. Kupferschmidt, K. (2019). Successful Ebola treatments promise to tame outbreak. *Science* 365, 628–629. <https://doi.org/10.1126/science.365.6454.628>.
 19. Troisi, M., Marini, E., Abbiento, V., Stazzoni, S., Andreano, E., and Rappuoli, R. (2022). A new dawn for monoclonal antibodies against antimicrobial resistant bacteria. *Front. Microbiol.* 13, 1080059. <https://doi.org/10.3389/fmicb.2022.1080059>.
 20. Andreano, E., Piccini, G., Licastro, D., Casalino, L., Johnson, N.V., Paciello, I., Dal Monego, S., Pantano, E., Manganaro, N., Manenti, A., et al. (2021). SARS-CoV-2 escape from a highly neutralizing COVID-19 convalescent plasma. *Proc. Natl. Acad. Sci. USA* 118, e2103154118. <https://doi.org/10.1073/pnas.2103154118>.
 21. Andreano, E., Nicastrì, E., Paciello, I., Pileri, P., Manganaro, N., Piccini, G., Manenti, A., Pantano, E., Kabanova, A., Troisi, M., et al. (2021). Extremely potent human monoclonal antibodies from COVID-19 convalescent patients. *Cell* 184, 1821–1835.e16. <https://doi.org/10.1016/j.cell.2021.02.035>.
 22. Severa, M., Diotti, R.A., Etna, M.P., Rizzo, F., Fiore, S., Ricci, D., Iannetta, M., Sinigaglia, A., Lodi, A., Mancini, N., et al. (2021). Differential plasmacytoid dendritic cell phenotype and type I interferon response in asymptomatic and severe COVID-19 infection. *PLoS Pathog.* 17, e1009878. <https://doi.org/10.1371/journal.ppat.1009878>.
 23. Vogelpoel, L.T.C., Baeten, D.L.P., de Jong, E.C., and den Dunnen, J. (2015). Control of cytokine production by human fc gamma receptors: implications for pathogen defense and autoimmunity. *Front. Immunol.* 6, 79. <https://doi.org/10.3389/fimmu.2015.00079>.
 24. Zhou, H., Møhlenberg, M., Thakor, J.C., Tuli, H.S., Wang, P., Assaraf, Y.G., Dhama, K., and Jiang, S. (2022). Sensitivity to Vaccines, Therapeutic Antibodies, and Viral Entry Inhibitors and Advances To Counter the SARS-CoV-2 Omicron Variant. *Clin. Microbiol. Rev.* 35, e0001422. <https://doi.org/10.1128/cmr.00014-22>.
 25. Gruell, H., Vanshylla, K., Korenkov, M., Tober-Lau, P., Zehner, M., Münn, F., Janicki, H., Augustin, M., Schommers, P., Sander, L.E., et al. (2022). SARS-CoV-2 Omicron sublineages exhibit distinct antibody escape patterns. *Cell Host Microbe* 30, 1231–1241.e6. <https://doi.org/10.1016/j.chom.2022.07.002>.
 26. Mackin, S.R., Desai, P., Whiteward, B.M., Karl, C.E., Liu, M., Baric, R.S., Edwards, D.K., Chiczy, T.M., McNamara, R.P., Alter, G., and Diamond, M.S. (2023). Fc-γR-dependent antibody effector functions are required for vaccine-mediated protection against antigen-shifted variants of SARS-CoV-2. *Nat. Microbiol.* 8, 569–580. <https://doi.org/10.1038/s41564-023-01359-1>.
 27. Zhang, A., Stacey, H.D., D’Agostino, M.R., Tugg, Y., Marzok, A., and Miller, M.S. (2023). Beyond neutralization: Fc-dependent antibody effector functions in SARS-CoV-2 infection. *Nat. Rev. Immunol.* 23, 381–396. <https://doi.org/10.1038/s41577-022-00813-1>.
 28. Torres, J.L., Ozorowski, G., Andreano, E., Liu, H., Coppes, J., Piccini, G., Donnici, L., Conti, M., Planchais, C., Planas, D., et al. (2022). Structural insights of a highly potent pan-neutralizing SARS-CoV-2 human monoclonal antibody. *Proc. Natl. Acad. Sci. USA* 119, e2120976119. <https://doi.org/10.1073/pnas.2120976119>.
 29. Alculumbre, S.G., Saint-André, V., Di Domizio, J., Vargas, P., Sirven, P., Bost, P., Maurin, M., Maiuri, P., Wery, M., Roman, M.S., et al. (2018). Diversification of human plasmacytoid dendritic cells in response to a single stimulus. *Nat. Immunol.* 19, 63–75. <https://doi.org/10.1038/s41590-017-0012-z>.
 30. Ren, X., Wen, W., Fan, X., Hou, W., Su, B., Cai, P., Li, J., Liu, Y., Tang, F., Zhang, F., et al. (2021). COVID-19 immune features revealed by a large-scale single-cell transcriptome atlas. *Cell* 184, 5838. <https://doi.org/10.1016/j.cell.2021.10.023>.
 31. Schulte-Schrepping, J., Reusch, N., Paclik, D., Baßler, K., Schlickeiser, S., Zhang, B., Krämer, B., Krammer, T., Brumhard, S., Bonaguro, L., et al. (2020). Severe COVID-19 Is Marked by a Dysregulated Myeloid Cell Compartment. *Cell* 182, 1419–1440.e23. <https://doi.org/10.1016/j.cell.2020.08.001>.
 32. Ricci, D., Etna, M.P., Severa, M., Fiore, S., Rizzo, F., Iannetta, M., Andreoni, M., Balducci, S., Stefanelli, P., Palamara, A.T., and Coccia, E.M. (2023). Novel evidence of Thymosin α1 immunomodulatory properties in SARS-CoV-2 infection: Effect on innate inflammatory response in a peripheral blood mononuclear cell-based in vitro model. *Int. Immunopharmacol.* 117, 109996. <https://doi.org/10.1016/j.intimp.2023.109996>.
 33. Lanini, S., Milleri, S., Andreano, E., Nosari, S., Paciello, I., Piccini, G., Gentili, A., Phogat, A., Hyseni, I., Leonardi, M., et al. (2022). Safety and serum distribution of anti-SARS-CoV-2 monoclonal antibody MAD0004J08 after intramuscular injection. *Nat. Commun.* 13, 2263. <https://doi.org/10.1038/s41467-022-29909-x>.
 34. Bruhns, P., Iannascoli, B., England, P., Mancardi, D.A., Fernandez, N., Jorieux, S., and Daëron, M. (2009). Specificity and affinity of human Fcγ receptors and their polymorphic variants for human IgG subclasses. *Blood* 113, 3716–3725. <https://doi.org/10.1182/blood-2008-09-179754>.
 35. Stapleton, N.M., Einarsson, H.K., Stemerding, A.M., and Vidarsson, G. (2015). The multiple facets of FcRn in immunity. *Immunol. Rev.* 268, 253–268. <https://doi.org/10.1111/imr.12331>.
 36. Foss, S., Watkinson, R., Sandlie, I., James, L.C., and Andersen, J.T. (2015). TRIM21: a cytosolic Fc receptor with broad antibody isotype specificity. *Immunol. Rev.* 268, 328–339. <https://doi.org/10.1111/imr.12363>.
 37. Benitez-Ribas, D., Tacken, P., Punt, C.J.A., de Vries, I.J.M., and Figdor, C.G. (2008). Activation of human plasmacytoid dendritic cells by TLR9 impairs Fc gammaRII-mediated

- uptake of immune complexes and presentation by MHC class II. *J. Immunol.* 181, 5219–5224. <https://doi.org/10.4049/jimmunol.181.8.5219>.
38. Tel, J., Sittig, S.P., Blom, R.A.M., Cruz, L.J., Schreibelt, G., Figdor, C.G., and de Vries, I.J.M. (2013). Targeting uptake receptors on human plasmacytoid dendritic cells triggers antigen cross-presentation and robust type I IFN secretion. *J. Immunol.* 191, 5005–5012. <https://doi.org/10.4049/jimmunol.1300787>.
 39. Björck, P., Beilhack, A., Herman, E.I., Negrin, R.S., and Engleman, E.G. (2008). Plasmacytoid dendritic cells take up opsonized antigen leading to CD4+ and CD8+ T cell activation *in vivo*. *J. Immunol.* 181, 3811–3817. <https://doi.org/10.4049/jimmunol.181.6.3811>.
 40. Sepulveda-Toepfer, J.A., Pichler, J., Fink, K., Sevo, M., Wildburger, S., Mudde-Boer, L.C., Taus, C., and Mudde, G.C. (2019). TLR9-mediated activation of dendritic cells by CD32 targeting for the generation of highly immunostimulatory vaccines. *Hum. Vaccin. Immunother.* 15, 179–188. <https://doi.org/10.1080/21645515.2018.1514223>.
 41. Dhodapkar, K.M., Banerjee, D., Connolly, J., Kukreja, A., Matayeva, E., Veri, M.C., Ravetch, J.V., Steinman, R.M., and Dhodapkar, M.V. (2007). Selective blockade of the inhibitory Fcγ receptor (FcγRIIB) in human dendritic cells and monocytes induces a type I interferon response program. *J. Exp. Med.* 204, 1359–1369. <https://doi.org/10.1084/jem.20062545>.
 42. Junqueira, C., Crespo, Â., Ranjbar, S., de Lacerda, L.B., Lewandrowski, M., Ingber, J., Parry, B., Ravid, S., Clark, S., Schrimpf, M.R., et al. (2022). FcγR-mediated SARS-CoV-2 infection of monocytes activates inflammation. *Nature* 606, 576–584. <https://doi.org/10.1038/s41586-022-04702-4>.
 43. Pitiot, A., Heuzé-Vourc'h, N., and Sécher, T. (2022). Alternative Routes of Administration for Therapeutic Antibodies-State of the Art. *Antibodies* 11, 56. <https://doi.org/10.3390/antib11030056>.
 44. Wilk, A.J., Rustagi, A., Zhao, N.Q., Roque, J., Martínez-Colón, G.J., McKechnie, J.L., Ivison, G.T., Ranganath, T., Vergara, R., Hollis, T., et al. (2020). A single-cell atlas of the peripheral immune response in patients with severe COVID-19. *Nat. Med.* 26, 1070–1076. <https://doi.org/10.1038/s41591-020-0944-y>.
 45. Rajamanickam, A., Kumar, N.P., Pandiarajan, A.N., Selvaraj, N., Munisankar, S., Renji, R.M., Venkatramani, V., Murhekar, M., Thangaraj, J.W.V., Kumar, M.S., et al. (2021). Dynamic alterations in monocyte numbers, subset frequencies and activation markers in acute and convalescent COVID-19 individuals. *Sci. Rep.* 11, 20254. <https://doi.org/10.1038/s41598-021-99705-y>.
 46. Ankerhold, J., Giese, S., Kolb, P., Maul-Pavicic, A., Voll, R.E., Göppert, N., Ciminski, K., Kreuz, C., Lothar, A., Salzer, U., et al. (2022). Circulating multimeric immune complexes contribute to immunopathology in COVID-19. *Nat. Commun.* 13, 5654. <https://doi.org/10.1038/s41467-022-32867-z>.
 47. Georg, P., Astaburuaga-García, R., Bonaguro, L., Brumhard, S., Michalick, L., Lippert, L.J., Kostevc, T., Gäbel, C., Schneider, M., Streitz, M., et al. (2022). Complement activation induces excessive T cell cytotoxicity in severe COVID-19. *Cell* 185, 493–512.e25. <https://doi.org/10.1016/j.cell.2021.12.040>.
 48. García-Nicolás, O., V'kovski, P., Zettl, F., Zimmer, G., Thiel, V., and Summerfield, A. (2021). No Evidence for Human Monocyte-Derived Macrophage Infection and Antibody-Mediated Enhancement of SARS-CoV-2 Infection. *Front. Cell. Infect. Microbiol.* 11, 644574. <https://doi.org/10.3389/fcimb.2021.644574>.
 49. Nichols, R.M., Macpherson, L., Patel, D.R., Yeh, W.W., and Peppercorn, A. (2024). Effect of Bamlanivimab as Monotherapy or in Combination with Etesevimab or Sotrovimab on Persistently High Viral Load in Patients with Mild-to-Moderate COVID-19: A Randomized, Phase 2 BLAZE-4 Trial. *Infect. Dis. Ther.* 13, 401–411. <https://doi.org/10.1007/s40121-024-00918-1>.
 50. Weinreich, D.M., Sivapalasingam, S., Norton, T., Ali, S., Gao, H., Bhowe, R., Musser, B.J., Soo, Y., Rofail, D., Im, J., et al. (2021). REGN-COV2, a Neutralizing Antibody Cocktail, in Outpatients with Covid-19. *N. Engl. J. Med.* 384, 238–251. <https://doi.org/10.1056/NEJMoa2035002>.
 51. Dougan, M., Azizad, M., Mocherla, B., Gottlieb, R.L., Chen, P., Hebert, C., Perry, R., Boscia, J., Heller, B., Morris, J., et al. (2022). A Randomized, Placebo-Controlled Clinical Trial of Bamlanivimab and Etesevimab Together in High-Risk Ambulatory Patients With COVID-19 and Validation of the Prognostic Value of Persistently High Viral Load. *Clin. Infect. Dis.* 75, e440–e449. <https://doi.org/10.1093/cid/ciab912>.
 52. Gottlieb, R.L., Nirula, A., Chen, P., Boscia, J., Heller, B., Morris, J., Huhn, G., Cardona, J., Mocherla, B., Stosor, V., et al. (2021). Effect of Bamlanivimab as Monotherapy or in Combination With Etesevimab on Viral Load in Patients With Mild to Moderate COVID-19: A Randomized Clinical Trial. *JAMA* 325, 632–644. <https://doi.org/10.1001/jama.2021.0202>.
 53. Sawant, J., Patil, A., and Kurl, S. (2023). A Review: Understanding Molecular Mechanisms of Antibody-Dependent Enhancement in Viral Infections. *Vaccines* (Basel) 11, 1240. <https://doi.org/10.3390/vaccines11071240>.
 54. Taylor, A., Foo, S.S., Bruzzone, R., Dinh, L.V., King, N.J.C., and Mahalingam, S. (2015). Fc receptors in antibody-dependent enhancement of viral infections. *Immunol. Rev.* 268, 340–364. <https://doi.org/10.1111/imr.12367>.
 55. Paciello, I., Maccari, G., Pantano, E., Andreano, E., and Rappuoli, R. (2024). High-resolution map of the Fc functions mediated by COVID-19-neutralizing antibodies. *Proc. Natl. Acad. Sci. USA* 121, e2314730121. <https://doi.org/10.1073/pnas.2314730121>.
 56. Robles, J.P., Zamora, M., Adan-Castro, E., Siqueiros-Marquez, L., Martínez de la Escalera, G., and Clapp, C. (2022). The spike protein of SARS-CoV-2 induces endothelial inflammation through integrin α5β1 and NF-κB signaling. *J. Biol. Chem.* 298, 101695. <https://doi.org/10.1016/j.jbc.2022.101695>.
 57. Montezano, A.C., Camargo, L.L., Mary, S., Neves, K.B., Rios, F.J., Stein, R., Lopes, R.A., Beattie, W., Thomson, J., Herder, V., et al. (2023). SARS-CoV-2 spike protein induces endothelial inflammation via ACE2 independently of viral replication. *Sci. Rep.* 13, 14086. <https://doi.org/10.1038/s41598-023-41115-3>.
 58. Trougakos, I.P., Terpos, E., Alexopoulos, H., Politou, M., Paraskevis, D., Scorilas, A., Kastritis, E., Andreacos, E., and Dimopoulos, M.A. (2022). Adverse effects of COVID-19 mRNA vaccines: the spike hypothesis. *Trends Mol. Med.* 28, 542–554. <https://doi.org/10.1016/j.molmed.2022.04.007>.
 59. Cosentino, M., and Marino, F. (2022). The spike hypothesis in vaccine-induced adverse effects: questions and answers. *Trends Mol. Med.* 28, 797–799. <https://doi.org/10.1016/j.molmed.2022.07.009>.
 60. Gallinaro, A., Borghi, M., Pirillo, M.F., Cecchetti, S., Bona, R., Canitano, A., Michelini, Z., Di Virgilio, A., Olvera, A., Brander, C., et al. (2020). Development and Preclinical Evaluation of an Integrase Defective Lentiviral Vector Vaccine Expressing the HIVACAT T Cell Immunogen in Mice. *Mol. Ther. Methods Clin. Dev.* 17, 418–428. <https://doi.org/10.1016/j.omtm.2020.01.013>.
 61. Borghi, M., Gallinaro, A., Pirillo, M.F., Canitano, A., Michelini, Z., De Angelis, M.L., Cecchetti, S., Tinari, A., Falce, C., Mariotti, S., et al. (2023). Different configurations of SARS-CoV-2 spike protein delivered by integrase-defective lentiviral vectors induce persistent functional immune responses, characterized by distinct immunogenicity profiles. *Front. Immunol.* 14, 1147953. <https://doi.org/10.3389/fimmu.2023.1147953>.

STAR★METHODS

KEY RESOURCES TABLE

REAGENT or RESOURCE	SOURCE	IDENTIFIER
Antibodies		
Mouse anti-human PD-L1 (alias B7-H1/CD274)-PeCy7	eBioscience	# 25-5983-71; RRID: AB_1907368
Mouse anti-human CD80-PE	BD Biosciences	# 557227; RRID: AB_396606
Mouse anti-human CD86-PE-CF594	BD Biosciences	# 562390; RRID: AB_11154047
Mouse anti-human CD14-eFluor780	eBioscience	# 47014942; RRID: AB_1834358
Mouse anti-human CD16-PE	BD Biosciences	# 561313; RRID: AB_10643606
Mouse anti-human CD32-APC	eBioscience	# 17-0329-41; RRID: AB_1272102
Mouse anti-human CD64-FITC	Beckman Coulter	# IM1604U; RRID: AB_395913
Mouse anti-human BDCA4 (alias CD304/Neuropilin-1) -APCR700	Miltenyi Biotech	# 130-090-533; RRID: AB_2744358
Fixable Viability Dye-eFluor450	eBioscience	# 65-0863-14
Human Fc gamma RI/CD64 Biotinylated Affinity Purified Pab	R&D Systems	# BAF1257
Human Fc gamma RII/CD32 Biotinylated Affinity Purified PAb (R&D Systems)	R&D Systems	# BAF1330
Human Fc gamma RIIB/CD16b Biotin Affinity Purified PAb (R&D Systems)	R&D Systems	# BAF1597
Bacterial and virus strains		
Clinical isolate of SARS-CoV-2 hCoV-19/Italy/LOM-ASST-CDG1/2020	Laboratory of Dr. Paola Stefanelli (ISS)	GISAID accession ID: EPI_ISL_412973
SARS-CoV-2 Omicron BA.1 variant	Laboratory of Prof. Rino Rappuoli (Fondazione Toscana Life Sciences)	GISAID ID: EPI_ISL_6794907
Biological samples		
PBMC of donor # 5 (male, 30 years old, caucasian)	This paper	N.A.
PBMC of donor # 6 (female, 38 years old, caucasian)	This paper	N.A.
PBMC of donor # 7 (female, 35 years old, caucasian)	This paper	N.A.
PBMC of donor # 12 (male, 52 years old, caucasian)	This paper	N.A.
PBMC of donor # 13 (female, 22 years old, caucasian)	This paper	N.A.
PBMC of donor # 33 (male, 52 years old, caucasian)	This paper	N.A.
PBMC of donor # 34 (female, 32 years old, caucasian)	This paper	N.A.
PBMC of donor # 35 (male, 41 years old, caucasian)	This paper	N.A.
PBMC of donor # 36 (male, 22 years old, caucasian)	This paper	N.A.
PBMC of donor # 37 (male, 48 years old, caucasian)	This paper	N.A.
PBMC of donor # 38 (male, 43 years old, caucasian)	This paper	N.A.
PBMC of donor # 39 (male, 51 years old, caucasian)	This paper	N.A.
PBMC of donor # 40 (female, 41 years old, caucasian)	This paper	N.A.
PBMC of donor # 41 (female, 54 years old, caucasian)	This paper	N.A.
PBMC of donor # 42 (male, 55 years old, caucasian)	This paper	N.A.
PBMC of donor # 55 (male, 43 years old, caucasian)	This paper	N.A.
PBMC of donor # 56 (male, 55 years old, caucasian)	This paper	N.A.
PBMC of donor # 60 (female, 28 years old, caucasian)	This paper	N.A.
PBMC of donor # 61 (female, 48 years old, caucasian)	This paper	N.A.
PBMC of donor # 62 (female, 54 years old, caucasian)	This paper	N.A.

(Continued on next page)

Continued

REAGENT or RESOURCE	SOURCE	IDENTIFIER
PBMC of donor # 63 (female, 48 years old, caucasian)	This paper	N.A.
PBMC of donor # 64 (male, 54 years old, caucasian)	This paper	N.A.
Chemicals, peptides, and recombinant proteins		
RPMI 1640 medium	Lonza	# BE12-167F
FBS	Euroclone	# ECS0186L
HEPES Buffer	Biowhittaker	# BE17-737E
Ficoll-Paque	Cedarlane	# CL5020
Trypsin EDTA	Biowhittaker	# BE17-161E
Non essential amino-acid	GIBCO	# 11140-035
PBS 1X, without calcium and magnesium	CORNING	# 21-031-CV
TLR7/8 agonist Resiquimod (R848)	Invivogen	#tlrl-r848
Formaldehyde solution	Sigma Aldrich	# 252549-1L
Biotinylated Recombinant SARS-CoV-2 Spike His-tag Avi-tag	R&D Systems	# AVI10549
Magnetic Beads™ Streptavidin	Acro Biosystems	# SMB-B01-10mg
Critical commercial assays		
Human Inflammatory Cytokine Cytometric Bead Array	BD Biosciences	# 551811
VeriKine Human Interferon Alpha Multi-Subtype ELISA Kit	PBL Assay Science	#41105-1
Human CD14 MicroBead Kit	Miltenyi Biotech	#130-050-201
Human CD304 (BDCA-4/Neuropilin-1) MicroBead Kit	Miltenyi Biotech	# 130-090-532
CalPhos™ Mammalian Transfection Kit	Clontech Laboratories	# 631312
Deposited data		
Human monoclonal antibody J08 and F05	https://doi.org/10.1016/j.cell.2021.02.035	Fondazione Toscana Life Sciences Italian patent applications n. 102020000015754 filed on June 30 th 2020, 102020000018955 filed on August 3 rd 2020 and 102020000029969 filed on 4 th of December 2020. International patent system number PCT/IB2021/055755 filed on the 28 th of June 2021
Experimental models: Cell lines		
Vero E6	ATCC	# CRL-1586
HEK 293T Lenti-X	Takara	# 632180
Recombinant DNA		
pCDNA3-SIVGagGFP	https://doi.org/10.1016/j.omtm.2020.01.013	N.A.
pSpike-C3	https://doi.org/10.3389/fimmu.2023.1147953	N.A.
Software and algorithms		
Cytextpert software (version 2.5)	Beckman Coulter	https://www.beckman.com/flow-cytometry/research-flow-cytometers/cytoflex/software
Prism software (version 9.4.1)	Graph Pad	https://www.graphpad.com/updates

(Continued on next page)

Continued

REAGENT or RESOURCE	SOURCE	IDENTIFIER
FCAP array software (version 3.0)	BD Biosciences	https://www.bdbiosciences.com/en-eu/products/instruments/software-informatics/instrument-software/fcap-array-software-v3-0.652099
Kaluza software (version 2.2)	Beckman Coulter	https://www.beckman.it/flow-cytometry/software/kaluza/downloads
Other		
Cytoflex LX cytometer	Beckman Coulter	https://www.beckman.it/flow-cytometry/research-flow-cytometers/cytoflex-lx
BD FACSCanto	BD Biosciences	https://www.bd.com/resource.aspx?idx=17867

RESOURCES AVAILABILITY

Lead contact

Further information and requests for resources and reagents should be directed to and will be fulfilled by the lead contact, Dr. Eliana M. Coccia (eliana.coccia@iss.it).

Materials availability

There are restrictions to the availability of the human monoclonal antibodies described in this study discovered, characterized and owned by Fondazione Toscana Life Sciences due to Italian patent applications n. 102020000015754 filed on June 30th 2020, 102020000018955 filed on August 3rd 2020 and 102020000029969 filed on 4th of December 2020, and international patent system number PCT/IB2021/055755 filed on the 28th of June 2021. Reasonable amounts of antibodies and plasmids will be made available by the owners upon request under a Material Transfer Agreement (MTA) for non-commercial usage.

Data and code availability

- The data reported in this paper will be shared by the [lead contact](#) upon request.
- This paper does not report original code.
- Any additional information required to reanalyze the data reported in this paper is available from the [lead contact](#) upon request.

EXPERIMENTAL MODEL AND STUDY PARTICIPANT DETAILS

Primary cultures of human origin

Primary cultures of human PBMC, pDC and monocytes were isolated from freshly collected buffy coats derived from blood donation of healthy volunteers of both sexes (Blood Bank of University "La Sapienza", Rome, Italy) that gave written informed consent.

Istituto Superiore di Sanità Review Ethic Board approved the use of blood from healthy volunteers for this study (AOO-ISS—14/ 06/2020–0020932). Sex, age and race of enrolled donors are reported in the [key resources table](#). Enrolled individuals were pseudo-anonymized; no other information including gender, ancestry, ethnicity or socioeconomic information was provided.

Vero E6 cells

Vero E6 cells (African green monkey kidney, Vero C1008, clone E6-CRL-1586; ATCC, not authenticated) were used for SARS-CoV-2 virus production and titration. Cell line was routinely tested for mycoplasma contamination.

293T Lenti-X cells

HEK 293T Lenti-X cells (Takara, #632180, not authenticated) a subclone of the transformed human embryonic kidney cell line HEK 293, which is highly transfectable and capable of producing high lentiviral titers, were used for production of Simian Immunodeficiency Virus (SIV)-based VLPs pseudotyped with SARS-CoV-2 S. Cell line was routinely tested for mycoplasma contamination.

Viral strains

Two SARS-CoV-2 strains were used in this study: the clinical isolate of SARS-CoV-2 hCoV-19/Italy/LOM-ASST-CDG1/2020 (GISAID accession ID: EPI_ISL_412973) and SARS-CoV-2 Omicron BA.1 variant (GISAID ID: EPI_ISL_6794907).

METHOD DETAILS

Isolation of PBMC, pDC and monocytes

PBMC were isolated from freshly collected buffy coats derived from blood donation of healthy volunteers (Blood Bank of University "La Sapienza", Rome, Italy) by density gradient centrifugation using lympholyte-H (Cedarlane, Hornby, Ontario, Canada).²²

pDC and monocytes were purified from isolated PBMC by magnetic separation by using anti-BDCA4 and anti-CD14 microbeads (Miltenyi biotech), respectively.²² The purity of the recovered cells was greater than 95% as assessed by flow cytometry analysis with anti-BDCA4 (Miltenyi biotech) or anti-CD14 (BD Biosciences) mAbs.

Virus production and titration

Virus was produced and titrated as followed.²² Briefly, Vero E6 (Vero C1008, clone E6-CRL-1586; ATCC) cells were cultured in Dulbecco's Modified Eagle Medium (DMEM) supplemented with non-essential amino acids (NEAA, 1x), penicillin/streptomycin (P/S, 100 U/mL), HEPES buffer (10 mM) and 10% (v/v) Fetal bovine serum (FBS). The clinical isolate of SARS-CoV-2 hCoV-19/Italy/LOM-ASST-CDG1/2020 (GISAID accession ID: EPI_ISL_412973, here called for simplicity D614G) and SARS-CoV-2 Omicron BA.1 variant (GISAID ID: EPI_ISL_6794907, here called for simplicity Omicron BA.1) were used.

Viral titer was determined by 50% tissue culture infective dose (TCID50) and plaque assay was used for confirming the obtained titer. SARS-CoV-2 stocks and supernatants of the different tested experimental conditions (see below) were titrated using End-point Dilutions Assay (EDA, TCID50/mL). Vero E6 cells (4 × 10⁵ cells/mL) were seeded into 96 wells plates and infected with base 10 dilutions of collected medium, each condition tested in triplicate. After 1 hour (h) of adsorption at 37°C, the cell-free virus was removed, and complete medium was added to cells. At 72 hpi, cells were observed to evaluate virus-induced cytopathic effect. TCID50/mL was calculated by Endpoint Dilution Assay by using the Reed-Muench formula.

Production and titration of VLPs

SIV-based VLPs pseudotyped with SARS-CoV-2 S were obtained by transient transfection on HEK 293T Lenti-X cells (Clontech) using plasmid pCDNA3-SIVGagGFP,⁶⁰ encoding the codon-optimized Gag protein from SIV fused to the GFP expressed from the Cytomegalovirus (CMV) promoter, to allow cytofluorimetric visualization of VLPs, and plasmid pSpike-C3,⁶¹ encoding the wt codon optimized SARS-CoV-2 S ORF (Wuhan-Hu-1, GenBank:NC_045512.2) with a 21 amino acid deletion at the cytoplasmic tail, to improve membrane tethering and pseudotyping. Briefly, 293T Lenti-X cells (3.5 × 10⁶ cells) were seeded on 10 cm Petri dishes (Corning Incorporated - Life Sciences) and transiently transfected with plasmids pCDNA3-SIVGagGFP (8 µg) and pSpike-C3 (3 µg) using the CalPhos™ Mammalian Transfection Kit (Clontech Laboratories). At 48 h post transfections, culture supernatants containing the VLPs SIVGagGFP/Spike were concentrated by ultracentrifugation on 20% sucrose cushion using a SW28 swinging bucket rotor (Beckman Coulter), resuspended in 1 X PBS and stored at -80°C until use. VLPs containing the GFP reporter fused to the carboxy-terminus of SIV-Gag protein were quantified by flow cytometry using a CytoFLEX LX flow cytometer (Beckman Coulter). PBS and non-fluorescent particles resuspended in PBS were used as negative controls to set the fluorescence threshold.

Cell stimulation

PBMC as well as isolated pDC and monocytes were pre-incubated for 1 h at 37°C with infectious D614G or Omicron BA.1, as specified in the figures, at a MOI of 0.04 and then cultured at 2 × 10⁶ cells/ml in RPMI 1640 in presence of P/S (100 U/mL), L-glutamine (2 mM) and 10% FBS for 24 h. Live SARS-CoV-2 was added alone or complexed with two classes of anti-SARS-CoV-2 Spike neutralizing IgG1 Abs (i.e. J08 and F05). After adsorption, cells were analyzed at 24 or 72 hpi. J08 and F05 nAbs were used as WT version, Fc MUT and as Fab truncated version²¹ at three increasing doses: one-tenth of the virus neutralizing dose assessed for both the nAbs at a concentration of 7.81 ng nAb/ml for 100 TCID50²⁰ (Dose N/10), the neutralizing dose itself (Dose N) and twice the neutralizing dose (Dose 2N).

Cells were also treated, where indicated, with the TLR-7/8 agonist Resiquimod (R848, 5 µM, Invivogen) and the TLR-9 ligand type C CpG (3 µg/ml, Invivogen) in presence or absence of increasing doses of J08 or F05 nAbs.

Viral uptake

PBMC were adsorbed for 1 h at 37°C with VLP (MOI=100) containing green-fluorescent protein (GFP) fused to Gag protein and pseudotyped with membrane-tethered D614G S protein alone or immunocomplexed with J08 nAbs in the WT or MUT versions at their neutralizing dose. Frequency of VLP-S-GFP+ cells was assessed by flow cytometry in gated viable and single cells after 10 minutes incubation with Trypsin-EDTA (Sigma Aldrich) to remove VLPs on the cell surface and to measure only the intracellular particles. Data were analyzed by a Cytoflex LX cytometer (Beckman Coulter) with Kaluza software (Beckman Coulter).

FcR crosslinking assay

Biotinylated recombinant trimeric S protein (SARS-CoV-2 Wuhan, 1 µg, R&D Systems) was coupled for 1 h at 37°C on a rocking plate to SA-labelled magnetic beads (1 µg, Acro Biosystems). IC were then formed leaving 1 h at 37°C WT J08 at the neutralizing dose with the biotinylated trimeric S alone or coupled to SA-magnetic beads. IC were then adsorbed to PBMC and cultured for 24 h to harvest culture supernatants.

As positive control biotinylated goat anti-human CD16 (FcγRIIIA/B), CD32 (FcγRII) and CD64 (FcγRI) Abs (anti-FcγR Abs, R&D Systems) were also coupled for 1 h to SA-magnetic beads and then mixed together in equal quantity (1 μg of each Ab coupled to 1 mg of SA-beads for total of 3 μg of Abs). Biotinylated goat anti-human immunoglobulin G (Isotype Ab, 3 μg, R&D Systems) coupled to SA-magnetic beads (1 mg) was used as negative control.

Detection of cytokines and chemokines in culture supernatants

Supernatants were harvested from PBMC, pDC and monocyte cultures at 24 and 72 hpi and treated for 30 minutes at 56°C to inactivate residual live virus prior of their storage at -80°C for later use.

Release of IFN-αs was measured by a specific ELISA kit (PBL assay science). Production of the cytokines IL-6 and TNF-α and of the chemokine IL-8 was quantified by specific cytometric bead array (BD Biosciences) on a FACS Canto (BD Biosciences) and analyzed by FCAP array software (BD Biosciences).

Flow cytometric analysis

Monoclonal Abs anti-PD-L1, CD80, CD86, CD14, CD16, CD32 and CD64 as well as IgG1 or IgG2a isotype controls were purchased from BD Biosciences, while anti-BDCA4 from Miltenyi Biotech. In particular, clones of mAbs used to study FcRs were chosen among those recognizing epitopes distal by the IC binding residues and that was not masked by the binding, i.e. clone B73.1 (BD Biosciences) for CD16, clone 7.5.4 (BD Biosciences) for CD32 and clone 22 (Beckman Coulter) for CD64. To establish cell viability and exclude dead cells from flow cytometry analyses, Fixable Viability Dye (FvDye, eBioscience) was always included in the mAb cocktails. Cells (10⁶ for monocytes or 2x10⁵ for pDC) were incubated with mAbs at 4°C for 30 min and then fixed with 4% paraformaldehyde before analysis on a Cytoflex LX cytometer (Beckman Coulter). Data were analyzed by Cytexpert software v.2.1 (Beckman Coulter). Expression of analyzed cell surface molecules was evaluated using the median fluorescence intensity (MFI). Only viable and single cells were considered for further analysis.

QUANTIFICATION AND STATISTICAL ANALYSIS

Statistical analysis was performed using One or Two-way Repeated-Measures ANOVA when three or more stimulation conditions were compared. In case of significant ANOVA, the pairwise comparisons were carried out using post-hoc approaches for multiple comparisons, to test the significance of the difference between two stimulation effects. Results were shown as median values ± Interquartile range (IQR). A p value ≤ 0.05 was considered statistically significant. In the figures, star scale was assigned as follows: * p ≤ 0.05; ** p ≤ 0.01. Data and statistical analyses were processed by Prism software version 9.4.1 (Graph Pad).